

# Theoretical Analysis of Exiting Sheet Thickness in Calendering of the Rabinowitsch Fluid

by

**Hira Siddique**



A dissertation submitted in partial fulfillment of the  
Degree of Masters of Philosophy in Mathematics

Supervised by

**Prof. Dr. Muhammad Sajid**

**School of Natural Sciences (SNS),**

National University of Sciences and Technology,

Islamabad, Pakistan.

**2016**

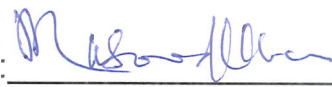

**National University of Sciences & Technology****MASTER'S THESIS WORK**

We hereby recommend that the dissertation prepared under our supervision by: Hira Siddique, Regn No. NUST201463628MSNS78014F Titled: Theoretical Analysis of Exiting Sheet Thickness in Calendering using Rabinowitsch Fluid be accepted in partial fulfillment of the requirements for the award of **MS** degree.

**Examination Committee Members**1. Name: Dr. Meraj Mustafa HashmiSignature: 2. Name: Dr. Muhammad Asif FarooqSignature: 

3. Name: \_\_\_\_\_

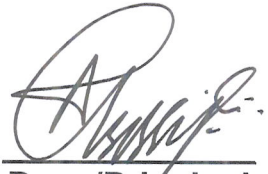
Signature: \_\_\_\_\_

4. Name: Dr. Masood KhanSignature: Supervisor's Name: Dr. Muhammad SajidSignature: 

Head of Department

14-10-2016

Date

**COUNTERSIGNED**Date: 14/10/16  
Dean/Principal

Dedicated to

**My family**

## *Acknowledgment*

First of all i would like to thank Allah (SWT) for His countless blessings and the strength and knowledge that He blessed me with to complete the commenced work.

I would like to express my sincere gratitude to my supervisor Dr. Muhammad Sajid Professor International Islamic University Islamabad (IIUI), for his unlimited support, sincere guidance and valuable advice and his precious time. His motivation and kind attitude helped me stay focused. I would like to especially thank him for being really patient throughout my research duration with him.

My Sincere gratitude to my GEC members Dr. Meraj Mustafa Hashmi (SNS) NUST and Dr. Asif Farooq (SNS) NUST for their valuable guidance and support that helped me complete my thesis in time.

My sincere regards to Dr. Nasir Ali Assistant Professor IIUI and Mr. Asif Javed Ph.D. Scholar IIUI for their assistance in my research publication and their valuable comments and advice in my research.

My heartiest and sincere salutations to my parents Mr. Siddique Ali Akbar and Mrs. Haleema Sadia for their endless support, love and prayers. I would also like to thank my siblings Mr. Hassan Siddique, Mr. Hussain Attique, Mr. Muhammad Mohsin and Mrs. Ammara Hassan for their continuous encouragement throughout the MS duration.

I would like to thank my friends Ms. Khadeeja Afzal, Ms. Rida Ahmad, Ms. Asma Masood, Ms. Sadia Khalid, Ms. Laraib Hanif for their continuous support and help during MS degree.

Hira Siddique

## Table of Contents

<b>Preface</b> .....	vii
<b>Chapter 1</b> .....	1
Preliminaries.....	1
<b>1.1 Fluid mechanics</b> .....	1
1.2 Classification of fluids.....	1
1.2.1 Newtonian fluids .....	1
1.2.2 Non-Newtonian fluids .....	2
1.3 Types of flow.....	4
1.3.1 Laminar flow .....	4
1.3.2 Turbulent flow .....	4
1.3.3 Uniform flow .....	4
1.3.4 Non-Uniform .....	4
1.3.5 Steady flow .....	5
1.3.6 Unsteady flow.....	5
1.3.7 Compressible Flow .....	5
1.3.8 Incompressible Flow .....	5
1.3.9 Rotational and irrotational flow.....	5
1.4 Basic assumptions of fluid flow .....	5
1.4.1 Conservation of mass .....	5
1.4.2 Conservation of momentum .....	6
1.4.3 Conservation of energy.....	7
1.5 Dimensionless numbers.....	7
1.5.1 Weissenberg number .....	7
1.5.2 Reynolds number.....	7
1.8 Calendering.....	7
1.8.1 Newtonian model of calendering.....	8
<b>Chapter 2</b> .....	12
<b>Theoretical analysis of the calendered exiting thickness of viscoelastic sheets</b> .....	12
2.1 Flow geometry.....	12

2.1.1	Governing equations.....	13
2.1.2	Dimensionless equations .....	14
2.2	Asymptotic solution for small Weissenberg number.....	17
2.2.1	Zeroth order solution .....	19
2.2.2	First order solution .....	20
2.3	Numerical solution .....	24
2.4	Results and Discussion .....	26
Chapter 3	.....	34
	Non-isothermal analysis of exiting sheet thickness in the calendering of Rabinowitsch fluid .....	34
3.1	Mathematical formulation .....	34
3.2	Results and conclusion .....	41
References	.....	52



## Preface

The calendering equipment was introduced in early 18<sup>th</sup> century by Edwin Chaffee and Charles Good year. However, a first theoretical analysis of calendering of the Newtonian and Bingham plastic materials was carried out by Gaskell [1]. The Gaskell analysis was based on the assumption of small rolls curvature. Later, Mckelvey [2] and Brazinsky et al. [3] reported a detailed analysis for power law fluids, which was followed by Alston and Astill [4] for a hyperbolic tangential fluid model. The analysis of Gaskell and Mckelvey was also reported by Middleman [5] and Tadmor and Gogos [6] in their text books on polymer processing. Experimental measurements of pressure profiles in calenders were conducted by Bergen and Scott [7]. Kiparissides and Vlachopoulos [8] carried out a finite element analysis of calendering without using the geometrical approximation and presented a comparison of their theoretical results with those obtained by Bergen and Scott [7]. It was concluded by them that for a power law fluid model, lower values of power law index reduce the disagreement between theory and experiments. In another attempt Kiparissides and Vlachopoulos [9] investigated non-isothermal flow of power law fluids in calendering process using finite element analysis. The geometrical assumptions in Gaskell [1] model were also dropped by Finston [10] using bipolar coordinates to represent the roll geometry. Apart from shear thinning models used in the above mentioned studies, viscoelastic fluids in calendering process were also considered by some authors. For instance, Paslay [11] used a three constants Oldroyd model in the calendering analysis. He emphasized on the interrelation of the parameters of the Oldroyd model with flow kinematics but neglected the normal stresses in the equation of motion. Tokita and White [12] utilized constitutive equation of second order Rivlin-Ericksen fluid to relate the experimental observation on calendering of elastomers to rheological parameters. Calendering was



analyzed by Chong [13] from hydrodynamic point of view for three constitutive equations namely; power law equation, Oldroyd-B equation and a modified second order equation. Sofou and Mitsoulis [14] provided numerical results for the viscoplastic calendering of sheets. All above mentioned studies were based on lubrication approximation theory (LAT). A numerical study of two dimensional flow in calendering process was carried out by Mitsoulis et al. [15] and Agassant and Espy [16]. More recently, Mitsoulis [17] numerically simulated the process of calendering viscoplastic sheets of finite thickness using finite element method. He concluded that LAT is good at predicting the detachment point, the pressure distribution and engineering quantities of interest.

It is a well-established fact that the inelastic models based on generalized Newtonian constitutive equations are not viscoelastic in the usual sense. This fact motivated Zhang and Tanner [18] to put forward a study based on Phan-Thien-Tanner fluid to analyze the calendering problem. They obtained solution to calendering problem using perturbation and finite element methods. Recently, Arcos et al. [19] reported a study on the influence of temperature-dependent consistency index on the exiting sheet thickness in the calendering process and they found a decrease of 6.91% for the calendered thickness. The influence of viscoelastic effects on the dimensionless exiting sheet thickness in the calendering process was also determined by Arcos et al. [20,21] using LAT. They found that an increase in the value of Weissenberg number tends to extend the length of contact between the rolls and the fluid. The ability of LAT in predicting accurately the quantities of engineering interest related to calendering motivated other researchers to analyze the calendering process. For, instance Siddiqui et al. [22] presented a perturbation analysis to study the calendering of non-Newtonian material characterized by a third-order fluid. Similarly, the constitutive equation of Casson model was utilized by Zahid et al. [23] to discuss the non-isothermal flow in a calender. More recently, Ali et al. studied the influence of viscoelastic effects on dimensionless exiting sheet thickness in the calendering using FENE-P fluid [24]. More recently Sajid et al. [25] provided an exact solution for the calendering analysis of a third order fluid. Motivated by these facts we have analyzed the flow and heat transfer analysis in calendering of a Rabinowitsch fluid in this dissertation.

The dissertation is structured as follows:

Chapter 1 deals with the basic definitions and notions. Calendering process is defined and its Newtonian case with the governing equations is enlightened.

Chapter 2 presents a detailed review of Arcos's work [20,21] on influence of viscoelastic effects on exiting sheet thickness during the calendering process, asymptotic and numerical solutions are reproduced and results are shown graphically.

Chapter 3 contains non-isothermal analysis of exiting sheet thickness in calendering of a Rabinowitsch fluid. The influence of involved parameter on velocity profile, pressure, pressure gradient, exiting sheet thickness and quantities of mechanical interest like force separating the two calenders and power transmitted to the fluid by the rolls is shown graphically. Moreover, the effects of viscous dissipation on calendering mechanism are also presented graphically.

# Chapter 1

## Preliminaries

This chapter is devoted to introduce the readers with the basics of fluid mechanics, governing equations and boundary conditions. We have taken most of the definitions from the book “Fluid Mechanics” by F.M. White and different sources on web.

### 1.1 Fluid mechanics

Fluid mechanics is a field of applied mechanics which deals with fluids in motion (Fluid Dynamics) and fluids at rest (Fluid Statics). The analysis of behavior of fluids is basically based on fundamental laws of mechanics, which relates conservation of mass and energy with force and momentum together with solid mechanics properties.

### 1.2 Classification of fluids

#### 1.2.1 Newtonian fluids

Based on their rheological behavior, fluids are classified as Newtonian and Non-Newtonian fluids. Fluids for which shear stress and deformation rate

are directly and linearly proportional are called Newtonian fluids. For unidirectional flow, this relation is expressed as:

$$\tau_{xy} = \mu \frac{du}{dy}, \quad (1.1)$$

where  $\tau_{xy}$  is the shear stress,  $\mu$  is shear rate viscosity and  $du/dy$  is the deformation rate.

## 1.2.2 Non-Newtonian fluids

Fluids for which the shear stress has a non-linear relation with deformation rate are called non-Newtonian fluids. For unidirectional flow, this relation can be expressed as

$$\tau_{xy} = \eta \frac{du}{dy}, \quad (1.2)$$

where  $\eta = k(du/dy)^{n-1}$  is the apparent viscosity, where  $k$  and  $n$  are respectively the consistency and flow behavior index. Non-Newtonian fluids are divided into three categories namely time dependent, time independent and viscoelastic fluids.

### 1.2.2.1 Time independent fluids

Most of the non-Newtonian fluids that we come across fit in this group. Apparent viscosity of this type of fluids only depends on shear stress knowing that the temperature is constant. Time independent fluids can be further subcategorized as under:

#### Pseudo-plastics

Pseudo-plastics are the ones for which apparent viscosity decreases as shear rate increases, also called shear thinning fluids. Some examples are blood and paints.

## **Dilatants**

Dilatants are the ones which has the reverse behavior to a pseudo-plastic fluid viz. its apparent viscosity increases as shear rate increases, also called shear thickening fluids. Thin paste of corn flour is a common example.

## **Viscoplastics**

Other than the above mentioned two types, there is another type of non-Newtonian fluids which does not behave as a fluid until a certain amount of shear stress, the yield stress, has been exceeded. Once this stress has been exceeded, viscosity either remains constant or decreases as shear rate increases. These materials are called viscoplastics. Some good examples are toothpaste and sewage sludge.

### **1.2.2.2 Time dependent fluids**

As the name illustrates, fluids that come under this category have apparent viscosity dependent on shear stress and on time as well for which shear stress is applied. Time dependent fluids can be subcategorized as under:

#### **Thixotropic fluids**

The thixotropic fluids are the ones for which apparent viscosity decreases with time under the action of a constant shear rate. Examples are honey, yogurt etc.

#### **Rheopectic fluids**

The rheopectic fluids are the ones for which apparent viscosity increases with time under the influence of constant shear rate. Examples are egg white and printing inks etc.

### **1.2.2.3 Viscoelastic fluids**

The materials which are neither purely elastic nor purely viscous are known as viscoelastic fluids. Materials which show the properties of both solids and liquids, they behave as solids or liquids depending on how long the stress is applied. It is often confused with plasticity. A viscoelastic material will return to its original shape after any deforming force is removed although it will take time to do so whereas a plastic material does not return to its original shape when the stress is removed.

## **1.3 Types of flow**

Flows are classified into following types,

### **1.3.1 Laminar flow**

A flow in which fluid particles move smoothly and regularly is said to be laminar. In this flow path of individual particles do not intersect with each other.

### **1.3.2 Turbulent flow**

A flow in which fluid particles move in irregular fashion in all directions is said to be turbulent. In this flow path of individual fluid particle intersect with each other.

### **1.3.3 Uniform flow**

A flow in which flow characteristics do not change from point to point is said to be uniform.

### **1.3.4 Non-Uniform**

A flow in which flow properties changes from point to point is said to be non-uniform.

### **1.3.5 Steady flow**

A flow is said to be steady in which fluid parameters or properties do not change with respect to time.

### **1.3.6 Unsteady flow**

The flow is said to be unsteady if the fluid parameters or properties changes with respect to time.

### **1.3.7 Compressible Flow**

If the volume of a given fluid particle varies with space and time i-e., density is function of space and time and no more constant, the flow becomes compressible. All gases are compressible fluids.

### **1.3.8 Incompressible Flow**

If the volume of a given fluid particle remains constant i-e., the density is constant, the flow is termed as incompressible flow. Generally all liquids are incompressible.

### **1.3.9 Rotational and irrotational flow**

If individual fluid particles rotate about their own axes during the flow, then flow is known as rotational. Otherwise, the flow is irrotational. Mathematically, for irrotational flow

$$\nabla \times V = 0. \quad (1.3)$$

## **1.4 Basic assumptions of fluid flow**

### **1.4.1 Conservation of mass**

The law of conservation of mass is given by

$$\frac{\partial \rho}{\partial t} + \nabla \cdot (\rho \mathbf{V}) = 0. \quad (1.4)$$

Also referred as continuity equation, where  $\rho$  is density of fluid and when density is constant continuity equation takes the form:

$$\nabla \cdot \mathbf{V} = 0. \quad (1.5)$$

In terms of Cartesian coordinate the component form of Eq. (1.5) is

$$\frac{\partial u}{\partial x} + \frac{\partial v}{\partial y} + \frac{\partial w}{\partial z} = 0, \quad (1.6)$$

where  $u, v$  and  $w$  are components of velocity in  $x, y$  and  $z$  directions respectively.

## 1.4.2 Conservation of momentum

Momentum remains conserved during flow and molecular collisions. Law of conservation of momentum takes the form:

$$\rho \frac{d\mathbf{V}}{dt} = \nabla \cdot \boldsymbol{\tau} + \rho \mathbf{b} - \nabla P, \quad (1.7)$$

where  $\rho \mathbf{b}$  gives net body force and  $d/dt = \partial/\partial t + (\mathbf{V} \cdot \nabla)$ . Momentum conservation equation in component form is as follow

$$\rho \left( \frac{du}{dt} \right) = -\frac{\partial P}{\partial x} + \frac{\partial \tau_{xx}}{\partial x} + \frac{\partial \tau_{xy}}{\partial y} + \frac{\partial \tau_{xz}}{\partial z}, \quad (1.8)$$

$$\rho \left( \frac{dv}{dt} \right) = -\frac{\partial P}{\partial y} + \frac{\partial \tau_{xy}}{\partial x} + \frac{\partial \tau_{yy}}{\partial y} + \frac{\partial \tau_{yz}}{\partial z}, \quad (1.9)$$

$$\rho \left( \frac{dw}{dt} \right) = -\frac{\partial P}{\partial z} + \frac{\partial \tau_{xz}}{\partial x} + \frac{\partial \tau_{yz}}{\partial y} + \frac{\partial \tau_{zz}}{\partial z}, \quad (1.10)$$

in  $x, y$  and  $z$  directions respectively.



### 1.4.3 Conservation of energy

Law of conservation of energy is given by

$$\rho c_p \left[ \frac{\partial T}{\partial t} + (\mathbf{V} \cdot \nabla) T \right] = k \nabla^2 T + \boldsymbol{\tau} : \mathbf{L}, \quad (1.11)$$

where  $T$  is temperature,  $k$  is thermal conductivity and  $L$  is the velocity gradient. In component form the heat equation for two dimensional flow takes the form

$$\begin{aligned} \frac{\partial T}{\partial t} + u \frac{\partial T}{\partial x} + v \frac{\partial T}{\partial y} = \frac{k}{\rho c_p} \left( \frac{\partial^2 T}{\partial x^2} + \frac{\partial^2 T}{\partial y^2} \right) + \frac{2\mu}{\rho c_p} \left\{ \left( \frac{\partial u}{\partial x} \right)^2 + \right. \\ \left. \left( \frac{\partial v}{\partial y} \right)^2 \right\} + \frac{\mu}{\rho c_p} \left\{ \left( \frac{\partial u}{\partial x} + \frac{\partial v}{\partial y} \right)^2 \right\}. \end{aligned} \quad (1.12)$$

## 1.5 Dimensionless numbers

### 1.5.1 Weissenberg number

The Weissenberg number  $Wi = \lambda_f U / H_0$  is a dimensionless number used in the study of viscoelastic flows and named after Karl Weissenberg. It is the ratio of the relaxation time of the fluid and a specific process time.

### 1.5.2 Reynolds number

Reynolds number is denoted by “ $Re$ ”, where  $Re = \rho U H_0 / \mu_0$  is the ratio of inertial force to the viscous force.

## 1.8 Calendering

The term “Calender” is derived from a Greek word *Kylindros* which means cylinder and according to the Webster’s International Dictionary, it means to press as cloth, rubber, paper between roller in order to make smooth and glossy.

Calendering is a process in which molten polymer is dragged through the narrow region between two corotating rolls in such a way as to produce a sheet of desired thickness. In an analysis of calendering process one seeks the expressions for velocity of the fluid, pressure gradient, pressure, exiting sheet thickness and some quantities of engineering interest.

### 1.8.1 Newtonian model of calendering

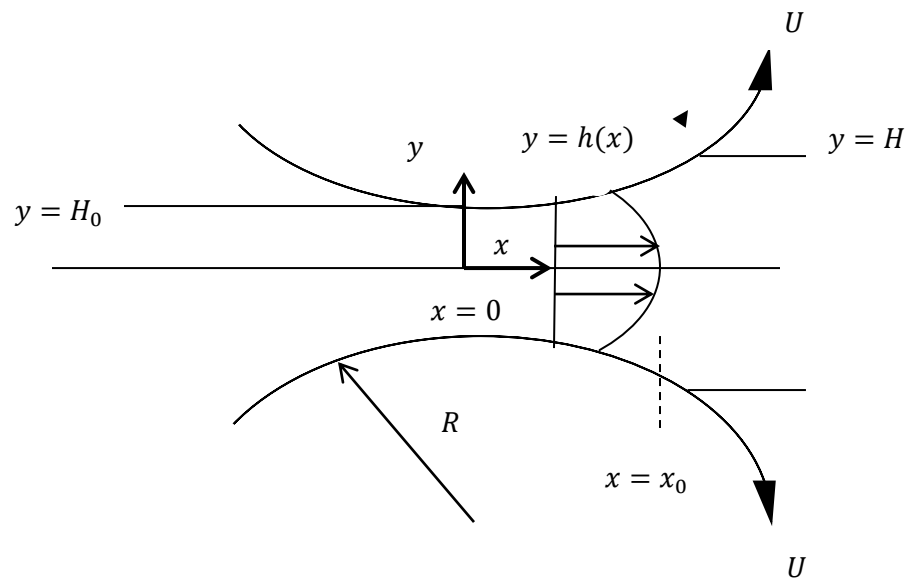


Fig. 1.1. Sketch for calender flow analysis.

The details of geometry and the flow field are shown in Fig. 1.1. Assuming that the flow is strictly two-dimensional, so that  $u = [u(x, y), v(x, y), 0]$ , the appropriate equations in steady state for an isothermal Newtonian fluid are

$$\frac{\partial u}{\partial x} + \frac{\partial v}{\partial y} = 0, \quad (1.13)$$

$$\rho u \frac{\partial u}{\partial x} + \rho v \frac{\partial u}{\partial y} = -\frac{\partial P}{\partial x} + \frac{\partial \tau_{yx}}{\partial y}, \quad (1.14)$$

$$\rho u \frac{\partial v}{\partial x} + \rho v \frac{\partial v}{\partial y} = -\frac{\partial P}{\partial y} + \frac{\partial \tau_{xy}}{\partial x}. \quad (1.15)$$

Our method will be to solve this problem by making some approximations that lead to a formulation involving only a single ordinary differential equation which can be solved easily. We begin with an argument that the most important dynamic events occur in the nip region. In this region and extending to either side by a distance of order of  $x_0$ , the roll surfaces are nearly parallel i.e.  $H_0 \ll R$ . It is convenient to say that flow is nearly parallel so that

$$u \ll v, \quad (1.16)$$

and

$$\frac{\partial}{\partial x} \ll \frac{\partial}{\partial y}. \quad (1.17)$$

Here we neglect inertial effects so Eqs. (1.13) and (1.14) become

$$-\frac{\partial P}{\partial x} + \mu \frac{\partial^2 u}{\partial y^2} = 0, \quad (1.18)$$

$$\frac{\partial P}{\partial y} = 0. \quad (1.19)$$

From above equation we can say that  $P$  is a function of  $x$  only so we can write

$$\frac{1}{\mu} \frac{dP}{dx} = \frac{\partial^2 u}{\partial y^2}. \quad (1.20)$$

The process that we did so far is often referred as using the famous lubrication approximation. Eq. (1.20) is easily integrated to arrive at

$$u = \frac{1}{2\mu} \frac{dP}{dx} y^2 + ay + b, \quad (1.21)$$

where  $a$  and  $b$  are constants of integration.

Here if we assume that both the rolls are identical and rotate with similar linear speed  $U$  then boundary conditions for this problem become

$$u = U \quad \text{at} \quad y = h(x), \quad (1.22)$$

$$\frac{\partial u}{\partial y} = 0 \quad \text{at} \quad y = 0. \quad (1.23)$$

By using these boundary conditions we get the constants of integration and Eq. (1.21) becomes

$$u = U + \frac{y^2 - h^2(x)}{2\mu} \frac{dP}{dx}. \quad (1.24)$$

The solution for  $u$  is still incomplete because  $u$  is a function of  $y$  explicitly and implicitly a function of  $x$  through  $h(x)$  and  $P(x)$ .

Here first we examine  $h(x)$ , the  $y$  distance from center line to the roll surface. It is easy to prove that

$$h = H_0 + R - (R^2 - x^2)^{1/2}. \quad (1.25)$$

Introducing the above relation into Eq. (1.24), complicates the problem so we will confine the analysis to value of  $x$ , such that  $x \ll R$ , so a good approximation to  $h(x)$  would be

$$h(x) = H_0 \left( 1 + \frac{x^2}{2H_0 R} \right). \quad (1.26)$$

Here we introduce dimensionless variables

$$x' = \frac{x}{\sqrt{2RH_0}}, \quad y' = \frac{y}{H_0}, \quad u' = \frac{u}{H}, \quad P' = \frac{PH_0}{\mu U}. \quad (1.27)$$

Then Eq. (1.24) becomes

$$u' = 1 + \sqrt{\frac{H_0}{8R}} [y'^2 - (1 + x'^2)^2] \frac{dP'}{dx'}. \quad (1.28)$$

Here we may find an expression for pressure gradient by using mass balance in the form

$$Q = 2 \int_0^h u dy = 2h(x) \left[ U - \frac{h^2(x)}{3\mu} \frac{dP'}{dx'} \right] = 1 + \lambda^2. \quad (1.29)$$

From above relation we can make  $dP'/dx'$  the subject as

$$\frac{dP'}{dx'} = \sqrt{\frac{18R}{H_0}} \frac{(x'^2 - \lambda^2)}{(1 + x'^2)^3}, \quad (1.30)$$

where a dimensionless flow rate  $\lambda$  has been introduced, which is defined as

$$\lambda^2 = \frac{Q}{2UH_0} - 1. \quad (1.31)$$

Thus we have replaced the unknown pressure gradient with known flow rate  $\lambda$ .

We shall describe calendaring process for some different fluids in later chapters.

# Chapter 2

## Theoretical analysis of the calendered exiting thickness of viscoelastic sheets

The chapter describes the detail review of work conducted by Arcos et al. [20] for the theoretical analysis of the calendering using a viscoelastic Simplified Phan-Thein-Tanner (SPTT) fluid model. The influence of viscoelastic effects on the dimensionless exiting sheet thickness in the calendering process are investigated. The physical laws of conservation of mass and momentum based on the lubrication theory were used. The quantities of engineering interest that includes the maximum pressure, the roll separating force and the power transmitted by the rolls is analyzed for various values of the viscoelastic parameter. In [20], the authors found an approximate solution of the velocity field and made all the proceeding analysis on the basis of that approximate velocity profile. We suggested the authors a correct expression of the velocity field and complete analysis of the results. In light of our correspondence with editor and author they have corrected their results in the form of a corrigendum and acknowledged our contribution [21].

### 2.1 Flow geometry

The physical model consists of two cylinders separated by a thin film of SPTT fluid are rotated in the opposite direction. Assuming  $R$  and  $\omega$  respectively be the radius and angular velocity of the cylinders. The linear velocity at the surface is thus  $U = \omega R$ , The minimum gap between the calenders,  $H_0$ , is such that  $H_0 \ll R$  and half of the exiting sheet thickness is represented as  $H$ . The geometry of

calender's surface is given as  $h(\bar{x}) = H_0(1 + \bar{x}^2/2RH_0)$ . The point where sheet first bites the rolls is represented by  $-\bar{x}_f$ . We must determine in the present analysis the unknown leave-off distance point of the sheet which is represented by  $\bar{x}_0$ . The symmetry of the problem allow us to consider only upper half of the configuration. We are taking coordinate system as shown in Fig. 2.1, where  $\bar{x}$  axis is taken in the direction of flow and  $\bar{y}$  points upwards, against the direction of gravity vector.

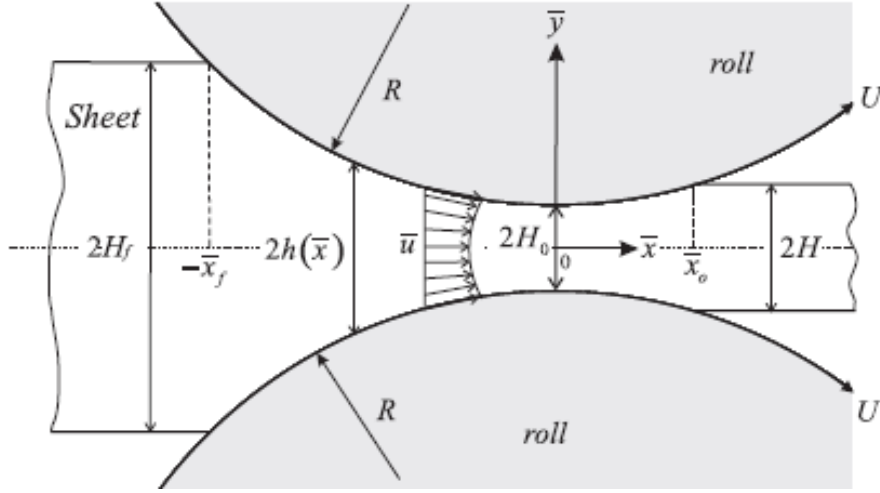


Fig. 2.1. Schematic diagram of the studied model in physical variables [20].

## 2.1.1 Governing equations

The equations that govern the present flow situation are

$$\frac{\partial \bar{u}}{\partial \bar{x}} + \frac{\partial \bar{v}}{\partial \bar{y}} = 0, \quad (2.1)$$

$$\rho \bar{u} \frac{\partial \bar{u}}{\partial \bar{x}} + \rho \bar{v} \frac{\partial \bar{u}}{\partial \bar{y}} = -\frac{\partial \bar{P}}{\partial \bar{x}} + \frac{\partial \bar{\tau}_{yx}}{\partial \bar{y}}, \quad (2.2)$$

$$\rho \bar{u} \frac{\partial \bar{v}}{\partial \bar{x}} + \rho \bar{v} \frac{\partial \bar{v}}{\partial \bar{y}} = -\frac{\partial \bar{P}}{\partial \bar{y}} + \frac{\partial \bar{\tau}_{xy}}{\partial \bar{x}}, \quad (2.3)$$

where  $\bar{u}$  and  $\bar{v}$  represent components of velocity in  $\bar{x}$  and  $\bar{y}$  direction respectively,  $\bar{P}$  is the pressure field and  $\bar{\tau}_{xy}$  is the shear stress. Constitutive equation for Simplified Phan-Thien-Tanner fluid [18] is given as:

$$\bar{\tau}_{xy} + \frac{2\epsilon\lambda_f^2}{\eta} \bar{\tau}_{xy}^2 \frac{\partial \bar{u}}{\partial \bar{y}} = \eta \frac{\partial \bar{u}}{\partial \bar{y}}, \quad (2.4)$$

where  $\epsilon$ ,  $\eta$  and  $\lambda_f$  represent elongation behavior of SPTT fluid model, polymer viscosity coefficient and relaxation time of the material, respectively.  $\eta$  is given by

$$\eta = \eta_0 \left( 1 + 2\epsilon\lambda_f^2 \left( \frac{\partial \bar{u}}{\partial \bar{y}} \right)^2 \right), \quad (2.5)$$

where  $\eta_0$  is zero shear rate viscosity. In the nip region and extending to either side, when  $H_0 \ll R$  roll surfaces are nearly parallel. So we can assume that flow is almost parallel, such that  $\bar{v} \ll \bar{u}$  and  $\frac{\partial \bar{u}}{\partial \bar{x}} \ll \frac{\partial \bar{u}}{\partial \bar{y}}$ . By this assumption, the boundary conditions associated to this problem take the form:

$$\bar{\tau}_{xy} = 0 \quad \text{at} \quad \bar{y} = 0, \quad (2.6)$$

$$\bar{u} = U \quad \text{at} \quad \bar{y} = h(\bar{x}). \quad (2.7)$$

## 2.1.2 Dimensionless equations

To make the equations dimensionless following new variables are introduced [20].

$$\begin{aligned} \chi &= \frac{\bar{x}}{\sqrt{2RH_0}}, \quad y = \frac{\bar{y}}{H_0}, \quad \frac{h(\bar{x})}{H_0} = 1 + \chi^2, \quad P = \frac{H_0 \bar{P}}{\mu_0 U} \sqrt{\frac{H_0}{2R}}, \\ \tau_{xy} &= \frac{H_0 \bar{\tau}_{xy}}{\mu_0 U}, \quad \lambda^2 = \frac{H}{H_0} - 1, \quad u(\chi, y) = \frac{\bar{u}(\bar{x}, \bar{y})}{U}, \end{aligned} \quad (2.8)$$



$$v(\chi, y) = \frac{\bar{v}(\bar{x}, \bar{y})}{U} \sqrt{\frac{2R}{H_0}}, \quad Q = \frac{\bar{Q}}{2UH_0}.$$

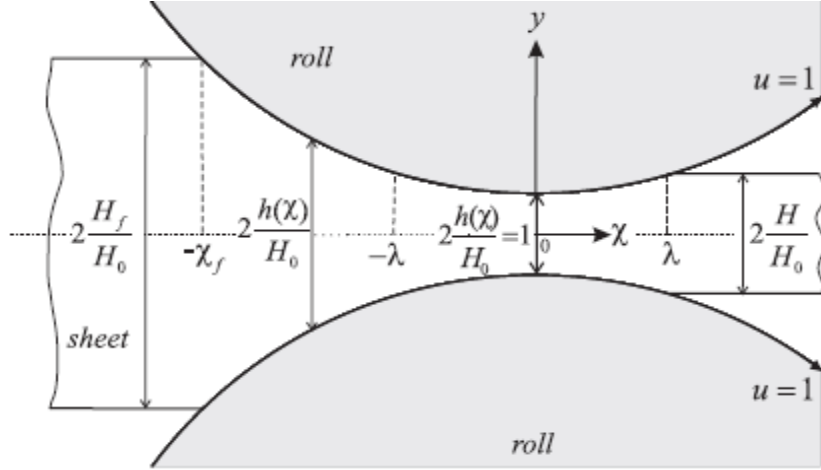


Fig. 2.2. Schematic diagram of physical model studied in dimensionless variables [20].

where  $Q$  is dimensionless volumetric flow rate, which is constant. Eqs (2.1) to (2.3) in dimensionless variables are

$$\frac{\partial u}{\partial \chi} + \frac{\partial v}{\partial y} = 0, \quad (2.9)$$

$$Re\beta \left( u \frac{\partial u}{\partial \chi} + v \frac{\partial u}{\partial y} \right) = -\frac{\partial P}{\partial \chi} + \frac{\partial \tau_{xy}}{\partial y}, \quad (2.10)$$

$$Re\beta^2 \left( u \frac{\partial v}{\partial \chi} + v \frac{\partial v}{\partial y} \right) = -\frac{\partial P}{\partial y} + \beta \frac{\partial \tau_{xy}}{\partial \chi}, \quad (2.11)$$

in which  $\beta = \sqrt{H_0/2R} \ll 1$ ,  $Re = \rho UH_0/\mu_0$ . In calendering process the Reynold's number is of the order of  $10^{-4} - 10^{-5}$  and therefore the inertia effects can be neglected. Invoking the lubrication theory Eqs. (2.10) and (2.11) yield

$$\frac{\partial P}{\partial y} \approx 0, \quad (2.12)$$

$$\frac{dP}{d\chi} = \frac{\partial \tau_{xy}}{\partial y}, \quad (2.13)$$

together with the dimensionless constitutive relationship

$$\tau_{xy} + 2\epsilon Wi^2 \tau_{xy}^2 \frac{\partial u}{\partial y} = \frac{\partial u}{\partial y}, \quad (2.14)$$

where  $Wi$  is the Weissenberg number, defined as  $Wi = \lambda_f U / H_0$ . In terms of new variables boundary conditions take the form

$$\tau_{xy} \Big|_{y=0} = 0, \quad (2.15)$$

$$u(y = 1 + \chi^2) = 1. \quad (2.16)$$

There are some additional conditions on pressure and pressure gradient in case of finite sheet examined here. It is assumed that pressure at the point where sheet first bites the rolls and the point where sheet leaves the rolls is zero. Pressure gradient is assumed to be zero at the exit point only. Mathematically, the dimensionless form of these conditions is given by

$$P(\chi = \lambda) = \frac{dP}{d\chi} \Big|_{\chi=\lambda} = 0, \quad (2.17)$$

$$P(\chi = -\chi_f) = 0. \quad (2.18)$$

It is clear from Eq. (2.12) that  $P$  is independent of  $y$  which allows integration of Eq. (2.13), so Eq. (2.13) give

$$\tau_{xy} = y \frac{dP}{d\chi} + C_1. \quad (2.19)$$

Utilizing the continuity condition gives  $C_1 = 0$ , therefore

$$\tau_{xy} = y \frac{dP}{d\chi}. \quad (2.20)$$

Substituting Eq. (2.20) into Eq. (2.14), we arrive at

$$y \frac{dP}{d\chi} + \frac{\partial u}{\partial y} \left( 2\epsilon Wi^2 y^2 \left( \frac{dP}{d\chi} \right)^2 - 1 \right) = 0, \quad (2.21)$$

along with Eq. (2.21) volumetric flow rate is required, which can be written in the form

$$Q = 1 + \lambda^2 = \int_0^{1+\chi^2} u dy, \quad (2.22)$$

where  $\lambda$  represent the exiting sheet thickness in the calendering and is given as

$$\lambda^2 = \frac{H}{H_0} - 1, \quad (2.23)$$

In the calendering analysis for Newtonian and non-Newtonian fluids, there are two flow regions, one in which pressure gradient is positive ( $-\chi_f \leq \chi \leq -\lambda$ ) and the other for which it is negative ( $-\lambda \leq \chi \leq \lambda$ ). Dimensionless pressure and velocity profiles are obtained here for each region.

## 2.2 Asymptotic solution for small Weissenberg number

We conduct an asymptotic solution of Eqs. (2.21) and (2.22) to obtain dimensionless pressure, velocity and leave-off distance of the finite sheet being examined. Applying the perturbation technique and using  $Wi^2$  as perturbation parameter, we can have the following expansions:

$$P(\chi) = P_0(\chi) + Wi^2 P_1(\chi) + \dots, \quad (2.24)$$

$$u(\chi, y) = u_0(\chi, y) + Wi^2 u_1(\chi, y) + \dots, \quad (2.25)$$

$$Q = Q_0 + Wi^2 Q_1 + \dots, \quad (2.26)$$

$$\lambda = \lambda_0 + Wi^2 \lambda_1 + \dots, \quad (2.27)$$

where  $P_0$ ,  $u_0$ ,  $Q_0$  and  $\lambda_0$  are the leading-order solutions, which refer to the Newtonian case.  $P_1$ ,  $u_1$ ,  $Q_1$  and  $\lambda_1$  are the first order terms and refer to the contribution of viscoelastic effects. Here it is important to mention that expansion (2.27) should be consistent with Eq. (2.25) in accordance with dimensionless volumetric flow rate per unit width discussed in eq. (2.22).

By introducing Eqs. (2.24)-(2.27) into Eqs. (2.12)-(2.22) and separating terms of the same powers of  $Wi^2$ , we get the following set of equations: lets say for  $(Wi^2)^0$ :

$$y \frac{dP_0}{d\chi} = \frac{\partial u_0}{\partial y}, \quad \text{for } -\chi_f \leq \chi \leq \lambda_0, \quad (2.28)$$

$$Q_0 = 1 + \lambda_0^2 = \int_0^{1+\chi^2} u_0 dy, \quad (2.29)$$

and the boundary conditions associated to Eqs. (2.28) and (2.29) are:

$$\tau_{xy_0} = 0 \quad \text{at } y = 0, \quad (2.30)$$

$$u_0 = 1 \quad \text{at } y = 1 + \chi^2, \quad (2.31)$$

$$P_0 = 0 \quad \text{at } \chi = -\chi_f, \quad (2.32)$$

$$P_0 = \frac{dP_0}{d\chi}, \quad \text{at } \chi = \lambda_0. \quad (2.33)$$

For the first order problem  $(Wi^2)^1$ :

$$y \frac{dP_1}{d\chi} - \frac{\partial u_1}{\partial y} + 2\epsilon \frac{\partial u_0}{\partial y} \left( \frac{dP_0}{d\chi} \right)^2 y^2 = 0 \quad \text{for } -\chi_f \leq \chi \leq \lambda_1, \quad (2.34)$$

$$Q_1 = 2\lambda_0\lambda_1 = \int_0^{1+\chi^2} u_1 dy. \quad (2.35)$$

In Arcos's analysis [20] it has been determined how  $\lambda$  is influenced by viscoelastic effects which was not studied before.

Boundary conditions associated with Eqs. (2.34) and (2.35) are:

$$\tau_{xy_1} = 0 \quad \text{at } y = 0, \quad (2.36)$$

$$u_1 = 0 \quad \text{at } y = 1 + \chi^2, \quad (2.37)$$

$$P_1 = 0 \quad \text{at } \chi = -\chi_f, \quad (2.38)$$

$$\frac{dP_1}{d\chi} = P_1 = 0 \quad \text{at } \chi = \lambda_1. \quad (2.39)$$

## 2.2.1 Zeroth order solution

For the case of finite sheet thickness, solution for Eqs. (2.28) and (2.29) is given by

$$u_0(y) = \frac{1}{2} \left( \frac{dP_0}{d\chi} \right) y^2 + C_2. \quad (2.40)$$

Using condition given is Eq. (2.31) we arrive at

$$u_0(y) = 1 + \frac{1}{2} \left( \frac{dP_0}{d\chi} \right) [y^2 - (1 + \chi^2)^2]. \quad (2.41)$$

Now using  $u_0(y)$  in Eq. (2.29) and equating to  $1 + \lambda^2$ . From which we make  $dP_0/d\chi$  subject as under

$$\frac{dP_0}{d\chi} = -3 \frac{(\lambda_0^2 - \chi^2)}{(1 + \chi^2)^3}, \quad \text{for} \quad -\chi_f \leq \chi \leq \lambda_0, \quad (2.42)$$

and after integrating Eq. (2.42) gives  $P_0(\chi)$ ,

$$P_0(\chi) = \frac{3}{8} \left( \frac{(1+3\lambda_0^2)}{1+\lambda_0^2} \lambda_0 + \chi \frac{(1+3\lambda_0^2)\chi^2 - 1 - 5\lambda_0^2}{(1+\chi^2)^2} + (1 - 3\lambda_0^2) [\tan^{-1} \chi - \tan^{-1} \lambda_0] \right). \quad (2.43)$$

Final sheet thickness, by using condition given in Eq. (2.33), is given by the following implicit relation.

$$\begin{aligned} & -\frac{2\lambda_0}{(1+\lambda_0^2)} + \left[ \frac{\lambda_0}{1+\lambda_0^2} + \tan^{-1} \lambda_0 \right] (1 - 3\lambda_0^2) - \\ & \left[ \frac{(H_f/H_0 - 1)^{1/2}}{H_f/H_0} + \tan^{-1} \left( \frac{H_f}{H_0} - 1 \right)^{1/2} \right] (1 - 3\lambda_0^2) + \\ & 2 \frac{(1+\lambda_0^2)(H_f/H_0 - 1)^{1/2}}{(H_f/H_0)^2} = 0. \end{aligned} \quad (2.44)$$

Here we can introduce a simple transformation for  $Y$  because of curvature of the rolls, which helps examine the velocity distribution i-e.,  $Y = y/(1 + \chi^2)$  in zeroth order velocity profile in Eq. (2.41) and substituting Eq. (2.42):

$$u_0 = 1 + \frac{3}{2} \left( \frac{\lambda_0^2 - \chi^2}{1 + \chi^2} \right) (1 - Y^2) \quad \text{for all} \quad \frac{dP_0}{d\chi}. \quad (2.45)$$

## 2.2.2 First order solution

In this section we obtain corrections to leading order solutions on dimensionless pressure and velocity profiles in a semi-analytical manner.

First we find  $u_1$  depending on  $dP_1/d\chi$  by substituting Eq. (2.42) and (2.44) into Eq. (2.34) we get:

$$y \frac{dP_1}{d\chi} - \frac{\partial u_1}{\partial y} + 2\epsilon y^2 \left( -3 \frac{(\lambda_0^2 - \chi^2)}{(1 + \chi^2)^3} \right)^2 \frac{\partial \left( 1 + \frac{3}{2} \left( \frac{\lambda_0^2 - \chi^2}{1 + \chi^2} \right) (1 - Y^2) \right)}{\partial y} = 0. \quad (2.46)$$

By introducing the transformation  $Y = \frac{y}{1 + \chi^2}$  to above equation and making  $\partial u_1 / \partial Y$  subject we get

$$\frac{\partial u_1}{\partial Y} = Y(1 + \chi^2)^2 \frac{dP_1}{d\chi} - 54\epsilon Y^3 \frac{(\lambda_0^2 - \chi^2)^3}{(1 + \chi^2)^5}. \quad (2.47)$$

Integrating above equation for  $u_1$  we get

$$u_1(\chi, Y) = \frac{1}{2} \frac{dP_1}{d\chi} (1 + \chi^2)^2 Y^2 - \frac{54}{4} \epsilon \frac{(\lambda_0^2 - \chi^2)^3}{(1 + \chi^2)^5} Y^4 + C_3(\chi), \quad (2.48)$$

using the boundary condition given in Eq. (2.37), we get the following form:

$$u_1(\chi, Y) = \frac{1}{2} \frac{dP_1}{d\chi} (1 + \chi^2)^2 (Y^2 - 1) - \frac{54}{4} \epsilon \frac{(\lambda_0^2 - \chi^2)^3}{(1 + \chi^2)^5} (Y^4 - 1). \quad (2.49)$$

To obtain first order of dimensionless volumetric flow rate, we need to evaluate Eq. (2.35) after substituting Eq. (2.49) and we get:

$$Q_1 = \frac{-1}{3} \frac{dP_1}{d\chi} (1 + \chi^2)^3 - \frac{54}{5} \epsilon \frac{(\chi^2 - \lambda_0^2)^3}{(1 + \chi^2)^4}. \quad (2.50)$$

Here we use the boundary condition given in Eq. (2.39) and we reach to the following form of first order volumetric flow rate.

$$Q_1 = -\frac{54}{5} \epsilon \frac{(\chi^2 - \lambda_0^2)^3}{(1 + \lambda_1^2)^4}. \quad (2.51)$$

By using Eq. (2.51) in Eq. (2.50) we obtain an explicit expression for  $\frac{dP_1}{d\chi}$

i-e.

$$\frac{dP_1}{d\chi} = \frac{162}{5} \epsilon \left[ \frac{(\lambda_1^2 - \lambda_0^2)^3}{(1+\chi^2)^3(1+\lambda_1^2)^4} - \frac{(\chi^2 - \lambda_0^2)^3}{(1+\chi^2)^7} \right]. \quad (2.52)$$

Eq. (2.52) is valid for  $-\chi_f \leq \chi \leq \lambda_1$ . The pressure distribution is obtained by integrating Eq. (2.52) as follow:

$$P_1(\chi) = \frac{162}{5} \epsilon \int_{-\chi_f}^{\chi} \left[ \frac{(\lambda_1^2 - \lambda_0^2)^3}{(1+\chi^2)^3(1+\lambda_1^2)^4} - \frac{(\chi^2 - \lambda_0^2)^3}{(1+\chi^2)^7} \right] d\chi. \quad (2.53)$$

After integration the first order dimensionless pressure becomes:

$$\begin{aligned} P_1(\chi) = \frac{162}{5} a & \left\{ \frac{\chi(1+3\lambda_0^2+3\lambda_0^4+\lambda_0^6)}{12(1+\chi^2)^6} + \frac{\chi(-25-39\lambda_0^2-3\lambda_0^4+11\lambda_0^6)}{120(1+\chi^2)^5} + \right. \\ & \frac{3\chi(15+\lambda_0^2-3\lambda_0^4+11\lambda_0^6)}{320(1+\chi^2)^4} + \frac{\chi(-5+21\lambda_0^2-63\lambda_0^4+231\lambda_0^6)}{1920(1+\chi^2)^3} + \\ & \frac{\chi(-5+21\lambda_0^2-63\lambda_0^4+231\lambda_0^6)}{1536(1+\chi^2)^2} + \frac{\chi(-5+21\lambda_0^2-63\lambda_0^4+231\lambda_0^6)}{1024(1+\chi^2)} + \\ & \frac{\chi(-\lambda_0^2+\lambda_1^2)^3}{4(1+\chi^2)^2(1+\lambda_1^2)^4} + \frac{3\chi(-\lambda_0^2+\lambda_1^2)^3}{8(1+\chi^2)(1+\lambda_1^2)^4} + \frac{3\text{ArcTan}[\chi](-\lambda_0^2+\lambda_1^2)^3}{8(1+\lambda_1^2)^4} + \\ & \frac{\text{ArcTan}[\chi](-5+21\lambda_0^2-63\lambda_0^4+231\lambda_0^6)}{1024} - \\ & \frac{3\text{ArcTan}\left[\sqrt{H_f/H_0-1}\right](-\lambda_0^2+\lambda_1^2)^3}{8(1+\lambda_1^2)^4} - \\ & \frac{\text{ArcTan}\left[\sqrt{H_f/H_0-1}\right](-5+21\lambda_0^2-63\lambda_0^4+231\lambda_0^6)}{1024} - \\ & \left. \sqrt{H_f/H_0-1} \left[ \frac{(1+3\lambda_0^2+3\lambda_0^4+\lambda_0^6)}{12(H_f/H_0)^6} + \frac{(-25-39\lambda_0^2-3\lambda_0^4+11\lambda_0^6)}{120(H_f/H_0)^5} + \right. \right. \\ & \left. \frac{3(15+\lambda_0^2-3\lambda_0^4+11\lambda_0^6)}{320(H_f/H_0)^4} + \frac{(-5+21\lambda_0^2-63\lambda_0^4+231\lambda_0^6)}{1920(H_f/H_0)^3} + \right. \end{aligned} \quad (2.54)$$



$$\left. \begin{aligned} & \frac{(-5+21\lambda_0^2-63\lambda_0^4+231\lambda_0^6)}{1536(H_f/H_0)^2} + \frac{(-5+21\lambda_0^2-63\lambda_0^4+231\lambda_0^6)}{1024(H_f/H_0)} + \\ & \left. \frac{(-\lambda_0^2+\lambda_1^2)^3}{4(H_f/H_0)^2(1+\lambda_1^2)^4} + \frac{3(-\lambda_0^2+\lambda_1^2)^3}{8(H_f/H_0)(1+\lambda_1^2)^4} \right\}. \end{aligned}$$

The dimensionless leave-off distance  $\lambda_1$  can be obtained by using the Eq. (2.53) along with the boundary condition given in Eq. (2.38)

$$0 = \int_{-\chi_f}^{\lambda_1} \left[ \frac{(\lambda_1^2 - \lambda_0^2)^3}{(1+\chi^2)^3(1-\lambda_1^2)^4} - \frac{(\chi^2 - \lambda_0^2)^3}{(1+\chi^2)^7} \right] d\chi. \quad (2.55)$$

$\lambda_1$  is given by the following implicit relation

$$\begin{aligned} 0 = & \sqrt{H_f/H_0} - 1 \left[ \frac{(1+3\lambda_0^2+3\lambda_0^4+\lambda_0^6)}{12(H_f/H_0)^6} + \frac{(-25-39\lambda_0^2-3\lambda_0^4+11\lambda_0^6)}{120(H_f/H_0)^5} + \right. \\ & \frac{3(15+\lambda_0^2-3\lambda_0^4+11\lambda_0^6)}{320(H_f/H_0)^4} + \frac{(-5+21\lambda_0^2-63\lambda_0^4+231\lambda_0^6)}{1920(H_f/H_0)^3} + \\ & \left. \frac{(-5+21\lambda_0^2-63\lambda_0^4+231\lambda_0^6)}{1536(H_f/H_0)^2} + \frac{(-5+21\lambda_0^2-63\lambda_0^4+231\lambda_0^6)}{1024(H_f/H_0)} + \right. \\ & \left. \frac{(-\lambda_0^2+\lambda_1^2)^3}{4(H_f/H_0)^2(1+\lambda_1^2)^4} + \frac{3(-\lambda_0^2+\lambda_1^2)^3}{8(H_f/H_0)(1+\lambda_1^2)^4} \right] + \frac{\lambda_1(1+3\lambda_0^2+3\lambda_0^4+\lambda_0^6)}{12(1+\lambda_1^2)^6} + \\ & \frac{\lambda_1(-25-39\lambda_0^2-3\lambda_0^4+11\lambda_0^6)}{120(1+\lambda_1^2)^5} + \frac{3\lambda_1(15+\lambda_0^2-3\lambda_0^4+11\lambda_0^6)}{320(1+\lambda_1^2)^4} + \\ & \frac{\lambda_1(-5+21\lambda_0^2-63\lambda_0^4+231\lambda_0^6)}{1920(1+\lambda_1^2)^3} + \frac{\lambda_1(-5+21\lambda_0^2-63\lambda_0^4+231\lambda_0^6)}{1536(1+\lambda_1^2)^2} + \\ & \frac{\lambda_1(-5+21\lambda_0^2-63\lambda_0^4+231\lambda_0^6)}{1024(1+\lambda_1^2)} + \frac{3\text{ArcTan}[\lambda_1](-\lambda_0^2+\lambda_1^2)^3}{8(1+\lambda_1^2)^4} + \\ & \frac{\text{ArcTan}[\lambda_1](-5+21\lambda_0^2-63\lambda_0^4+231\lambda_0^6)}{1024} + \\ & \frac{3\text{ArcTan}\left[\sqrt{H_f/H_0-1}\right](-\lambda_0^2+\lambda_1^2)^3}{8(1+\lambda_1^2)^4} + \\ & \frac{\text{ArcTan}\left[\sqrt{H_f/H_0-1}\right](-5+21\lambda_0^2-63\lambda_0^4+231\lambda_0^6)}{1024} + \frac{\lambda_1(-\lambda_0^2+\lambda_1^2)^3}{4(1+\lambda_1^2)^4} + \end{aligned} \quad (2.56)$$

$$\frac{3\lambda_1(-\lambda_0^2+\lambda_1^2)^3}{8(1+\lambda_1^2)^5}.$$

For a given value of  $H_f/H_0$  its corresponding  $\lambda_0$  and  $\lambda_1$  can be calculated using Eqs. (2.44) and (2.56) respectively.

## 2.3 Numerical solution

To determine the dimensionless pressure, velocity profiles and leave-off distance of the finite sheet being examined here, we present the numerical solution of Eqs. (2.20) and (2.21) here:

For this purpose we integrate Eq. (2.20) with respect to  $y$  to find an explicit expression for velocity profile  $u$  depending on pressure gradient

$$u = -\frac{\ln[1-2\epsilon(dP/d\chi)^2Wi^2y^2]}{4\epsilon(dP/d\chi)Wi^2} + C. \quad (2.57)$$

Using condition in eq. (2.16),  $u$  becomes

$$u = \frac{\ln[(1-2\epsilon(dP/d\chi)^2Wi^2(1+\chi^2)^2)/(1-2\epsilon(dP/d\chi)^2Wi^2y^2)]}{4\epsilon(dP/d\chi)Wi^2} + 1. \quad (2.58)$$

Eq. (2.58) is the correct expression for the velocity  $u$  which we proposed to the authors to correct their analysis [21]. The volumetric flow rate is given by

$$Q = 1 + \lambda^2 = \int_0^{1+\chi^2} \left[ \frac{\ln[(1-2\epsilon(dP/d\chi)^2Wi^2(1+\chi^2)^2)/(1-2\epsilon(dP/d\chi)^2Wi^2y^2)]}{4\epsilon(dP/d\chi)Wi^2} + 1 \right] dy, \quad (2.59)$$

$$1 + \lambda^2 = (1 + \chi^2) - \frac{(1+\chi^2)}{2\epsilon(dP/d\chi)Wi^2} + \frac{\tanh^{-1}[\sqrt{2\epsilon}Wi(dP/d\chi)(1+\chi^2)]}{2\sqrt{2}(\epsilon)^{3/2}(dP/d\chi)^2Wi^3}. \quad (2.60)$$

Now pressure gradient has an implicit expression as follows:

$$\frac{dP}{d\chi} = \frac{\tanh^{-1}[\sqrt{2\epsilon}Wi(dP/d\chi)(1+\chi^2)] - (1+\chi^2)\sqrt{2\epsilon}Wi(dP/d\chi)}{2\sqrt{2}(\epsilon)^{3/2}(\lambda^2 - \chi^2)Wi^3(dP/d\chi)}. \quad (2.61)$$

Therefore the pressure distribution can be given as:

$$P(\chi) = \int_{\lambda}^{\chi} \frac{\tanh^{-1}[\sqrt{2\epsilon}Wi(dP/d\chi)(1+\chi^2)] - (1+\chi^2)\sqrt{2\epsilon}Wi(dP/d\chi)}{2\sqrt{2}(\epsilon)^{3/2}(\lambda^2 - \chi^2)Wi^3(dP/d\chi)} d\chi. \quad (2.62)$$

Now Eq. (2.61) is an implicit expression for pressure gradient, which we can determine for given values of  $Wi$ , and for assumed values of  $\lambda$ , the leave-off distance as a function of dimensionless longitudinal coordinate  $\chi$ . The local solution is obtained numerically by modified false position method [27]. After that local pressure is found by using Runge-Kutta algorithm by integrating  $dP/d\chi$ , from  $\chi = \lambda$  and using pressure boundary conditions mentioned in Eq. (2.17). The extrema of pressure profile occurs at  $\chi = \pm\lambda, -\chi_f$ . For a given value of dimensionless leave-off distance Eq. (2.61) is integrated till the pressure becomes negative. Here we have found the point where sheet first bites the rolls  $-\chi_f$  from which we can find the entering sheet thickness from the relation:

$$\chi_f = \sqrt{H/H_0 - 1}. \quad (2.63)$$

The force -separating two rolls is of importance to the mechanical design of calendering system and to the prediction of film thickness uniformity. It can be determined by integrating pressure over area of interest on surface of the roll.

$$\frac{F}{W} (Wi) = \frac{\mu_0 U}{H_0} \mathfrak{S}(Wi), \quad (2.64)$$

where  $\mathfrak{S}(\alpha)$  is given by

$$\mathfrak{S}(Wi) = 6 \int_{-\chi_f}^{\lambda} \left[ \int_{\chi}^{\lambda} \Gamma(Wi) d\chi \right] d\chi, \quad (2.65)$$

where

$$\Gamma(Wi) = \left[ \frac{\tanh^{-1}[\sqrt{2\epsilon Wi}(dP/d\chi)(1+\chi^2)] - (1+\chi^2)\sqrt{2\epsilon Wi}(dP/d\chi)}{2\sqrt{2}(\epsilon Wi)^{3/2}(\lambda^2 - \chi^2)} \right]^{1/2}. \quad (2.66)$$

The total power input into both rolls can now be computed by integrating product of roll velocity and shear stress along surface of roll.

$$\dot{W}(Wi) = WU^2 \mu_0 \sqrt{\frac{R}{H_0}} \wp(Wi), \quad (2.67)$$

where the dimensionless power function is given by:

$$\wp(Wi) = -6\sqrt{2} \int_{-\chi_f}^{\lambda} \Gamma(Wi) Ad\chi. \quad (2.68)$$

## 2.4 Results and Discussion

The numerical results for SPTT fluid model are presented here. Figs. 2.3 and 2.5 show the dimensionless pressure gradient for different values of Weissenberg number  $Wi = 0.1, 6, 9$ , as a function of dimensionless axial coordinates  $\chi$  for two fixed values of leave-off distance  $\lambda = 0.2923, 0.440$ . We can see that at  $\chi = \pm\lambda$ , pressure gradient passes the axial coordinate and its value is minimum for  $\chi = 0$ , it has both increasing and decreasing trend along the flow region. Pressure gradient is decreasing when  $\chi$  leaves  $\lambda$ , decreases until the minimum then increases and becomes zero again at  $\chi = -\lambda$ , and keeps increasing until the maximum value arrives then again decreases until the entering point  $-\chi_f$  is reached where sheet bites the rolls in the first place. We can note here

that for a fixed value of  $\lambda$ , as  $Wi$  increases it tends to increase the domain. Also at  $\chi = 0$ , varying  $Wi$  strongly affect pressure gradient because deformation rate has maximum negative value here. At  $\chi = \pm\lambda$  flat velocity profiles are reached so  $Wi$  has smaller effect there.

In Figs. 2.4 and 2.6 dimensionless pressure distribution is shown, for varying  $Wi$ , as a function of  $\chi$ , which we have obtained from Eq. (2.62). Starting from right, at  $\chi = \lambda$  pressure increases to a maximum value at  $\chi = -\lambda$  and decrease to zero till the entry point  $\chi = -\chi_f$  is reached. We can see that pressure is strongly affected by varying  $Wi$  at  $\chi = -\lambda$ .

In Figs. 2.7 and 2.8 velocity profile is presented as function of  $Y$  for different values of Weissenberg number. Dimensionless velocity profiles are evaluated at two different values of  $\chi$ . Velocity profile as shown in Fig. 2.7 is plotted in the region  $-\chi_f \leq \chi \leq -\lambda$  where the pressure gradient is positive. We can notice that  $u$  increases as Weissenberg number increases for a given value of  $\lambda$ . Velocity profile is also plotted in the region  $-\lambda \leq \chi \leq \lambda$ , where we can see in Fig. 2.8 velocity profiles decrease as Weissenberg number increases.

In Fig. 2.9 dimensionless leave-off distance  $\lambda$  is presented as a function of entering sheet thickness  $H_f/H_0$  for different values of Weissenberg number. Here we know that we have assumed  $\lambda$  to be known and we have to calculate  $\chi_f$  by using the relationship given in Eq. (2.63).

Roll separating force and the power input to the fluid by the rolls is plotted as a function of Weissenberg number by varying dimensionless leave-off distance  $\lambda$  using the relation described in Eqs. (2.65) and (2.68). In Fig. 2.10 we observe that force separating the two rolls decreases as Weissenberg number increases for two different values of dimensionless leave-off distance  $\lambda$  ( $=0.470, 0.475$ ). Power is also a decreasing function

of Weissenberg number and is plotted in Fig. 2.11 for different values of  $\lambda$ (=0.2923, 0.470, 0.475).

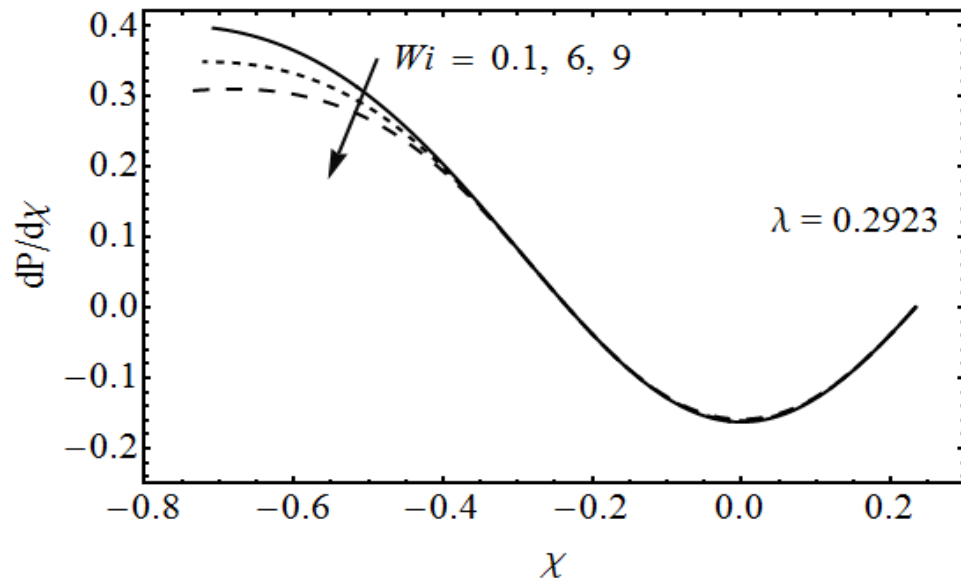


**Fig. 2.3.** The dimensionless pressure gradient for SPTT fluid model, for varying Weissenberg number.  $\lambda = 0.2923$ .

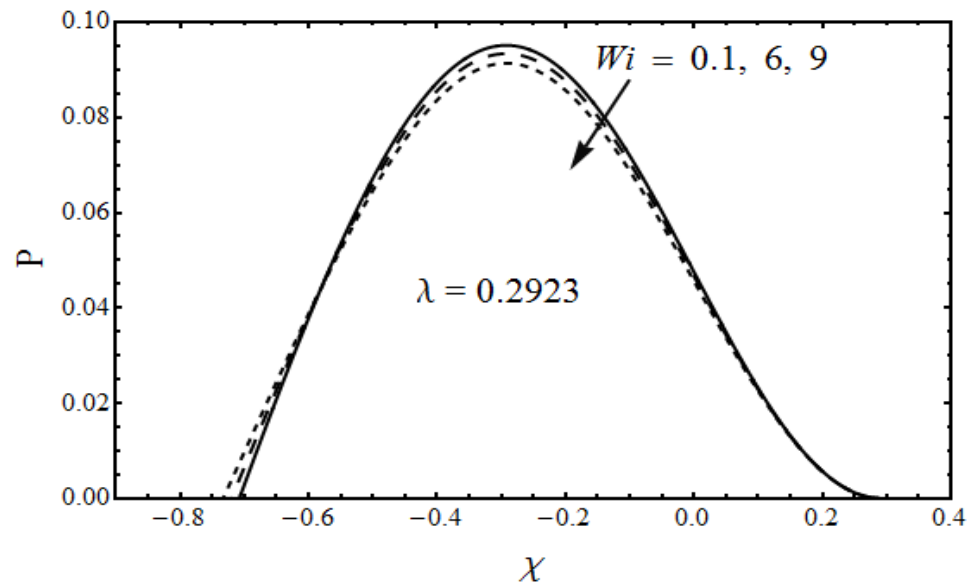


**Fig. 2.4.** The Dimensionless pressure profile, in gap along the flow region, for varying Weissenberg number.  $\lambda = 0.2923$ .

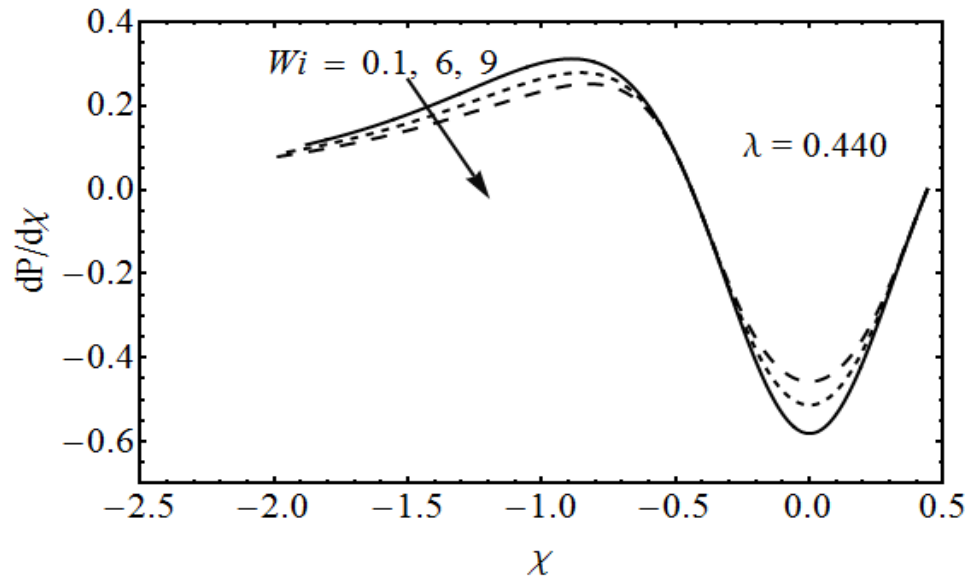


**Fig. 2.5.** The dimensionless pressure gradient for SPTT fluid model, for varying Weissenberg number.  $\lambda = 0.440$ .

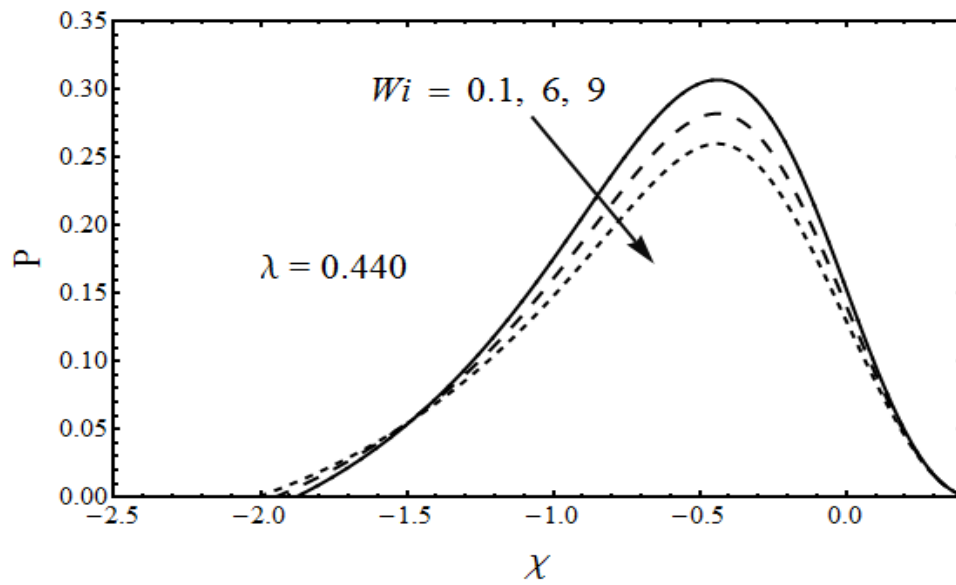


**Fig. 2.6.** The dimensionless pressure profile, in gap along the flow region, for varying Weissenberg number.  $\lambda = 0.440$ .



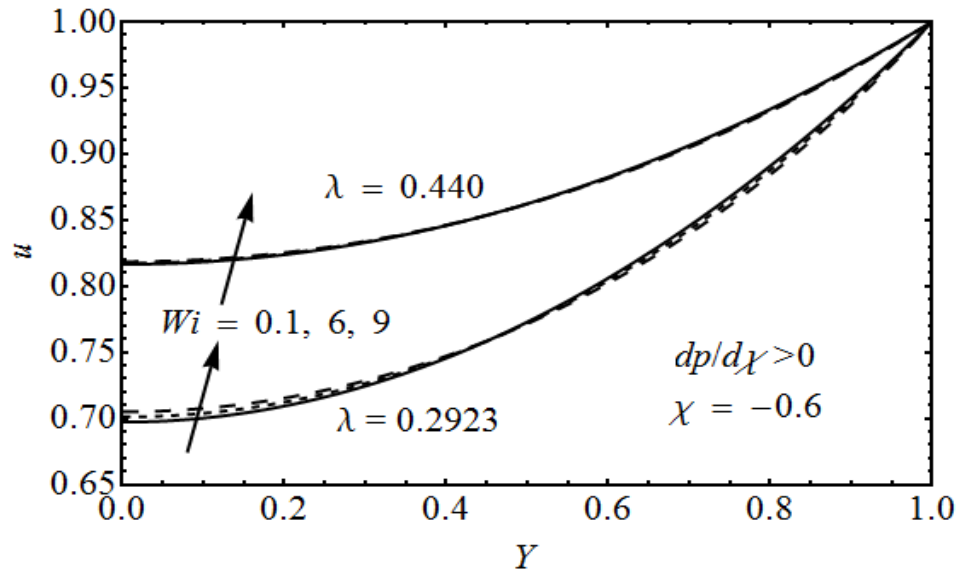


**Fig. 2.7.** The Dimensionless velocity profile  $u$  as a function of transversal coordinate  $Y$ , for varying Weissenberg number, evaluated at  $\chi = -0.6$  for  $\lambda = 0.440, 0.2923$ .

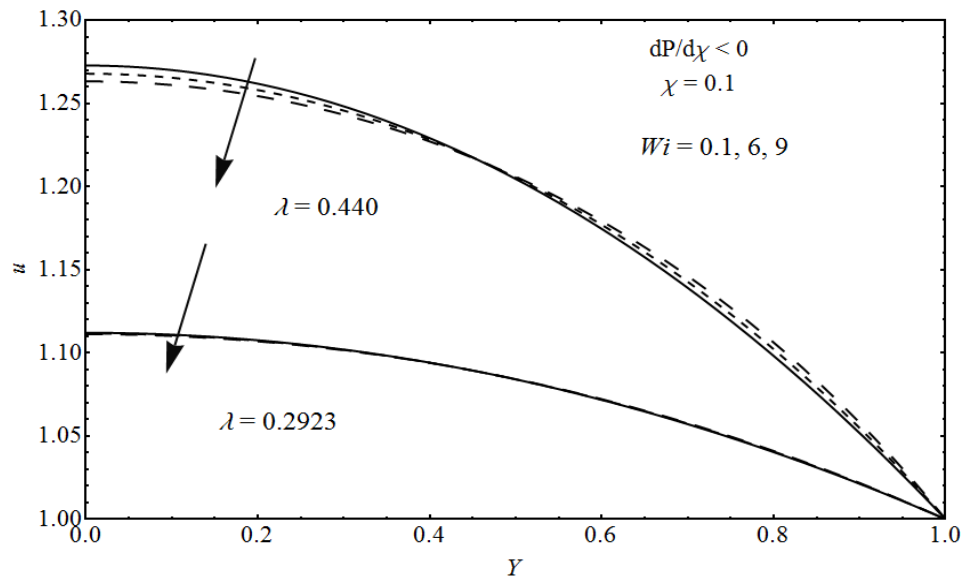


**Fig. 2.8.** The Dimensionless velocity profile  $u$  as a function of transversal coordinate  $Y$ , for varying Weissenberg number, evaluated at  $\chi = 0.1$  for  $\lambda = 0.440, 0.2923$ .

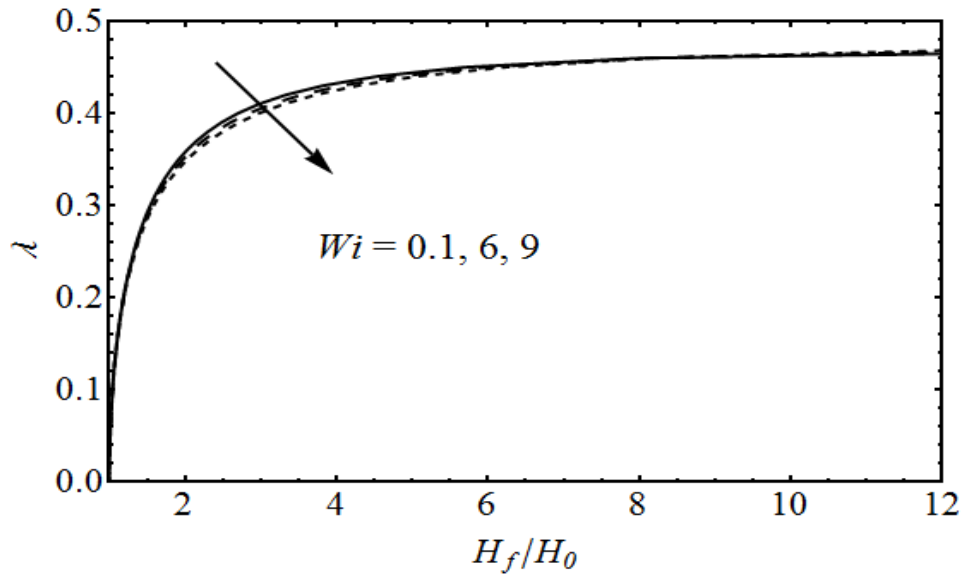


**Fig. 2.9.** The dimensionless leave-off distance as a function of entering sheet thickness for varying Weissenberg number.

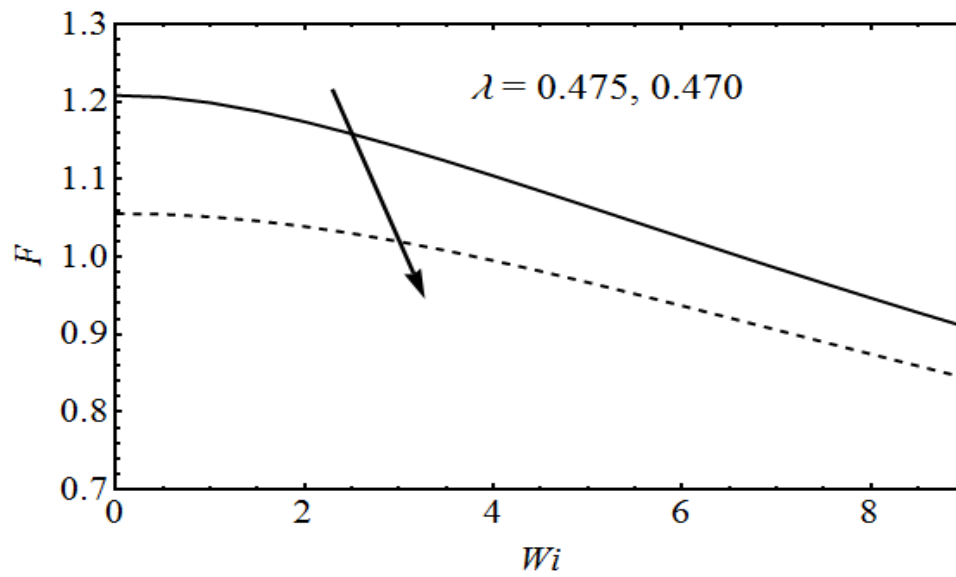


**Fig. 10.** Force as function of Weissenberg number, in terms of  $\lambda$ .

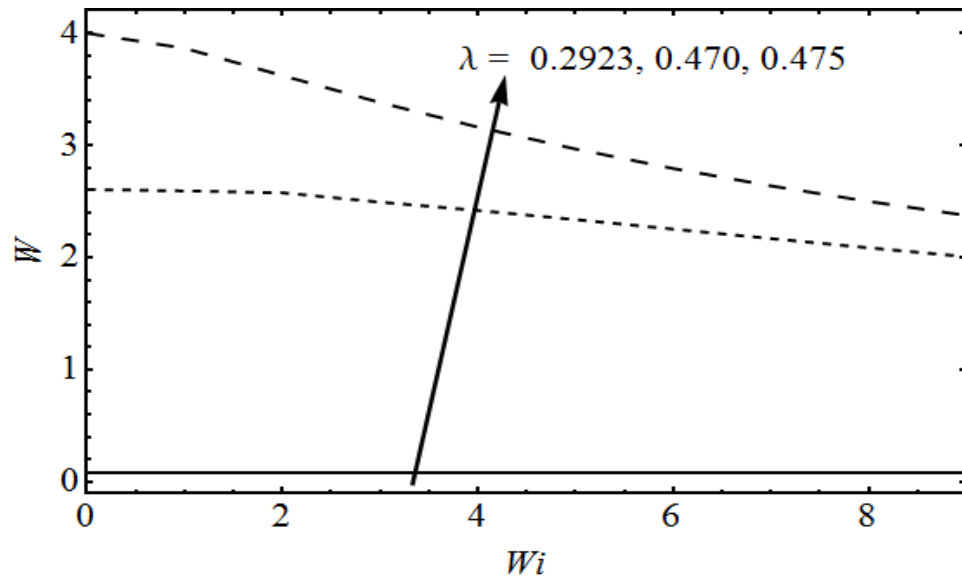


**Fig. 11.** Power as function of Weissenberg number, in terms of  $\lambda$ .

## **Chapter 3**

### **Non-isothermal analysis of exiting sheet thickness in the calendering of Rabinowitsch fluid**

The focus of the present chapter is to utilize the constitutive relationship of a Rabinowitsch fluid to discuss the calendering. The analysis of heat transfer is also included in this chapter. Rabinowitsch fluid is a special kind of non-Newtonian fluid which exhibits pseudo-plastic behavior for certain values of non-linearity factor and behaves as dilatant for another set of values of the non-linearity parameter. Based on Rabinowitsch constitutive relationship quantities of engineering interest are evaluated and analyzed.

#### **3.1 Mathematical formulation**

The physical model is same as discussed in the previous chapter. Equations that govern the flow and heat transfer in the calendering process are given in Eqs. (2.1)-(2.3) together with energy equation

$$\rho c_p \left( \bar{u} \frac{\partial T}{\partial \bar{x}} + \bar{v} \frac{\partial T}{\partial \bar{y}} \right) = k \left( \frac{\partial^2 T}{\partial \bar{x}^2} + \frac{\partial^2 T}{\partial \bar{y}^2} \right) + \bar{\tau}_{xy} \frac{\partial \bar{u}}{\partial \bar{y}}, \quad (3.1)$$

where  $k$  is the thermal conductivity and  $c_p$  is the specific heat.

Rabinowitsch fluid obeys the following constitutive relationship

$$\bar{\tau}_{xy} + \gamma \bar{\tau}_{xy}^3 = \mu \frac{\partial \bar{u}}{\partial \bar{y}}, \quad (3.2)$$

where  $\gamma$  is the non-linear factor responsible for non-Newtonian effects of fluids and is called coefficient of pseudoplasticity.

Boundary conditions for velocity are same as in Eqs. (2.15)-(2.18).

However for temperature we have

$$T(\bar{x}, \bar{y}) = T_0 \quad \text{at} \quad \bar{y} = h(\bar{x}), \quad (3.3)$$

$$T(\bar{x}, \bar{y}) = T_0 \quad \text{at} \quad \bar{y} = h(\bar{x}), \quad (3.4)$$

$$T(\bar{x}, \bar{y}) = T_0 \quad \text{at} \quad \bar{x} = -\bar{x}_f. \quad (3.5)$$

In terms of dimensionless variables defined in Eq. (2.8) together with

$$\theta(\chi, y) = \frac{T(\bar{x}, \bar{y}) - T_0}{\Delta T_c}, \quad (3.6)$$

$$\alpha = \frac{\gamma \mu_0^2 U^2}{H_0^2}, \quad (3.7)$$

we have

$$\tau_{xy} + \alpha \tau_{xy}^3 = \frac{\partial u}{\partial y}. \quad (3.8)$$

Invoking the lubrication approximation the problem takes the form

$$\frac{\partial P}{\partial \chi} = \frac{\partial \tau_{xy}}{\partial y}, \quad (3.9)$$

$$\frac{\partial P}{\partial y} = 0, \quad (3.10)$$

$$u = 1, \quad \theta(\chi, y) = 0 \quad \text{at} \quad y = 1 + \chi^2, \quad (3.11)$$

$$\tau_{xy} = 0, \quad \frac{\partial \theta}{\partial y} = 0 \quad \text{at} \quad y = 0, \quad (3.12)$$

$$\theta(\chi, y) = 0 \quad \text{at} \quad \chi = -\chi_f, \quad (3.13)$$

and

$$Gz u \frac{\partial \theta}{\partial \chi} = \frac{\partial^2 \theta}{\partial y^2} + Br \tau_{xy} \frac{\partial u}{\partial y}, \quad (3.14)$$

where  $G_z = \sqrt{\frac{H_0}{2R} \frac{e c_p U H_0}{k}}$  and  $Br = \frac{\mu U^2}{k \Delta T_c}$ .

$$\frac{dP}{d\chi} = 0 = P \quad \text{at} \quad \chi = \lambda, \quad (3.15)$$

$$P = 0 \quad \text{at} \quad \chi = -\chi_f. \quad (3.16)$$

From (3.10) we know that  $P$  is independent of  $y$  so by integrating Eq. (3.9) and using boundary condition Eq. (3.12) we get

$$\tau_{xy} = y \frac{dP}{d\chi}. \quad (3.17)$$

Substituting Eq. (3.17) into Eq. (3.8) we obtain

$$y \frac{dP}{d\chi} + \alpha y^3 \frac{dP^3}{d\chi} - \frac{\partial u}{\partial y} = 0. \quad (3.18)$$

We also need dimensionless volumetric flow rate which can be written in the form:

$$Q = 1 + \lambda^2 = \int_0^{1+\chi^2} u dy. \quad (3.19)$$

The Eqs. (3.18) and (3.19) represent lubrication approximation for viscoelastic fluids. The parameter  $\lambda$  has been extensively studied in past for the case where viscoelastic effects were not considered [1, 5, 26].

By integrating Eq. (3.18) with respect to  $y$  we get:

$$u(y) = \frac{1}{2} \frac{dP}{d\chi} (y^2 - (1 + \chi^2)^2) + \frac{\alpha}{4} \frac{dP^3}{d\chi} (y^4 - (1 + \chi^2)^4) + 1. \quad (3.20)$$

Substituting  $u(y)$  in Eq. (3.19) and integrating it we get and then equating to  $1 + \lambda^2$  after using condition given in Eq. (3.15)

$$\frac{\alpha}{4} (1 + \chi^2)^5 \frac{dP^3}{d\chi} + \frac{1}{3} (1 + \chi^2)^3 \frac{dP}{d\chi} + \lambda^2 - \chi^2 = 0. \quad (3.21)$$

From Eq. (3.21) we get an explicit expression for  $dP/d\chi$ , i-e

$$\frac{dP}{d\chi} = \frac{1}{3} \left\{ - \frac{2.2^{\frac{2}{3}} A^3}{[-27\alpha^2 A^{10} B + \sqrt{16\alpha^3 A^{24} + 729\alpha^4 A^{20} B^2}]^{\frac{1}{3}}} + \frac{\frac{1}{2^{\frac{1}{3}} [-27\alpha^2 A^{10} B + \sqrt{16\alpha^3 A^{24} + 729\alpha^4 A^{20} B^2}]^{\frac{1}{3}}}}{\alpha A^5} \right\}, \quad (3.22)$$

where  $A = (1 + \chi^2)$  and  $B = (\lambda^2 - \chi^2)$  Now we can also write expression for  $P(\chi)$  as follow:

$$P(\chi) = \int_{\lambda}^{\chi} \left\{ \frac{1}{3} \left( - \frac{2.2^{\frac{2}{3}} A^3}{[-27\alpha^2 A^{10} B + \sqrt{16\alpha^3 A^{24} + 729\alpha^4 A^{20} B^2}]^{\frac{1}{3}}} + \frac{\frac{1}{2^{\frac{1}{3}} [-27\alpha^2 A^{10} B + \sqrt{16\alpha^3 A^{24} + 729\alpha^4 A^{20} B^2}]^{\frac{1}{3}}}}{\alpha A^5} \right) \right\} d\chi. \quad (3.23)$$

Following Arcos et. al. [20] we use a simple transformation that helps to examine the dimensionless velocity distribution that is  $Y = y/A$ .

$$u(Y) = \frac{1}{2} \frac{dP}{d\chi} A^2 (Y^2 - 1) + \frac{\alpha}{4} \frac{dP^3}{d\chi} A^4 (Y^4 - 1) + 1. \quad (3.24)$$

Now the integration  $\int dP/d\chi$  is difficult to perform analytically so by using Mathematica built-in function “NIntegrate”, integration of Eq. (3.23) is carried out for dimensionless leave off distance  $\chi = \lambda$  corresponding to finite sheet thickness until pressure becomes negative. This process is also explained by J. C. Arcos [20]. Corresponding value of  $\chi$  where pressure crosses the x axis is noted as  $\chi = -\chi_f$  where the entering sheet first bites the rolls and from this thickness of entering sheet can be determined by  $\chi_f = \left(\frac{H_f}{H_0} - 1\right)^{\frac{1}{2}}$ .

The force separating two rolls is of importance to the mechanical design of calendaring system and to the prediction of film thickness uniformity. It can be determined by integrating pressure over area of interest on surface of the roll.

$$\frac{F}{W}(\alpha) = \frac{\mu_0 U}{H_0} \mathfrak{S}(\alpha), \quad (3.25)$$

where  $\mathfrak{S}(\alpha)$  is given by

$$\mathfrak{S}(\alpha) = 6 \int_{-\chi_f}^{\lambda} \left[ \int_{\chi}^{\lambda} \Gamma(\alpha) d\chi \right] d\chi, \quad (3.26)$$

where

$$\Gamma(\alpha) = \frac{1}{3} \left\{ - \frac{2.2^{\frac{2}{3}} A^3}{[-27\alpha^2 A^{10} B + \sqrt{16\alpha^3 A^{24} + 729\alpha^4 A^{20} B^2}]^{\frac{1}{3}}} + \right. \quad (3.27)$$



$$\left. \frac{\frac{1}{2^{\frac{1}{3}}[-27\alpha^2 A^{10} B + \sqrt{16\alpha^3 A^{24} + 729\alpha^4 A^{20} B^2}]^{\frac{1}{3}}}}{\alpha A^5} \right\}$$

The total power input into both rolls can now be computed by integrating product of roll velocity and shear stress along surface of roll.

$$\dot{W}(\alpha) = WU^2 \mu_0 \sqrt{\frac{R}{H_0}} \wp(\alpha), \quad (3.28)$$

where the dimensionless power function is given by:

$$\wp(\alpha) = -6\sqrt{2} \int_{-\chi_f}^{\lambda} \Gamma(\alpha) A d\chi. \quad (3.29)$$

The energy equation in terms of  $Y$  is given by

$$\frac{\partial^2 \theta}{\partial Y^2} = Gz(1 + \chi^2)^2 u \frac{\partial \theta}{\partial \chi} - Br(1 + \chi^2)^2 Y \frac{dP}{d\chi} \frac{\partial u}{\partial y}, \quad (3.30)$$

$$\theta(\chi, Y) = 0 \quad \text{at} \quad Y = 1, \quad (3.31)$$

$$\frac{\partial \theta(\chi, Y)}{\partial Y} = 0 \quad \text{at} \quad Y = 0, \quad (3.32)$$

$$\theta(\chi, Y) = 0 \quad \text{at} \quad \chi = -\chi_f. \quad (3.33)$$

Substituting expressions for  $u$  we have

$$\begin{aligned} \frac{\partial^2 \theta}{\partial Y^2} = Gz \frac{(1+\chi^2)^4}{2} \left[ \frac{dP}{d\chi} (Y^2 - 1) + \frac{\alpha(1+\chi^2)^2}{2} \frac{dP^3}{d\chi} (Y^4 - 1) + \right. \\ \left. 1 \right] \frac{\partial \theta}{\partial \chi} - Br(1 + \chi^2)^2 Y^2 \left( \frac{dP}{d\chi} \right)^2 \left[ 1 + \alpha(1 + \chi^2)^2 Y^2 \left( \frac{dP}{d\chi} \right)^2 \right]. \end{aligned} \quad (3.34)$$

Eq. (3.34) is a partial differential equation in space coordinates and its challenging to find its analytical solution. To handle this situation, we chose to simulate this problem numerically using the hybrid technique. The hybrid technique is based on the finite difference method and shooting algorithm.

This technique is based on the following steps

We first substitute  $\partial\theta/\partial\chi = (\theta_i - \theta_{i-1})/\Delta\chi$  by using finite difference formula. By using this expression in Eq. (3.34), the resulting equation and boundary conditions at *ith* step are given in the following form.

$$\frac{\partial^2\theta}{\partial Y^2} = GZ \frac{(1+\chi_i^2)^4}{2} \left[ \frac{dP}{d\chi} (Y^2 - 1) + \frac{\alpha(1+\chi_i^2)^2}{2} \left( \frac{dP}{d\chi} \right)^3 (Y^4 - 1) + 1 \right] \frac{(\theta_i - \theta_{i-1})}{\Delta\chi} - Br(1 + \chi_i^2)^2 Y^2 \left( \frac{dP}{d\chi} \right)^2 \left[ 1 + \alpha(1 + \chi_i^2)^2 Y^2 \left( \frac{dP}{d\chi} \right)^2 \right], \quad (3.35)$$

$$\frac{\partial\theta(\chi, 0)}{\partial Y} = 0, \quad (3.36)$$

$$\theta_i(\chi_i, 1) = 0. \quad (3.37)$$

Now Eq. (3.35) with boundary conditions Eqs. (3.36) and (3.37) can be solved using shooting method for each *i*. For this purpose we reduced the above equation into system of first order differential equations.

Let

$$\theta_i = f_i, \quad (3.38)$$

$$\frac{\partial\theta_i}{\partial Y} = \frac{\partial f_i}{\partial Y} = g_i, \quad (3.39)$$

$$\frac{\partial g_i}{\partial Y} = GZ \frac{(1+\chi_i^2)^4}{2} \left[ \frac{dP_i}{d\chi_i} (Y^2 - 1) + \frac{\alpha(1+\chi_i^2)^2}{2} \left( \frac{dP_i}{d\chi_i} \right)^3 (Y^4 - 1) + 1 \right] \frac{(f_i - f_{i-1})}{\Delta\chi} - Br(1 + \chi_i^2)^4 Y^2 \left( \frac{dP_i}{d\chi_i} \right)^2 \left[ 1 + \alpha(1 + \chi_i^2)^2 Y^2 \left( \frac{dP_i}{d\chi_i} \right)^2 \right], \quad (3.40)$$

$$f_i(\chi_i, 0) = s_i, \quad (3.41)$$

$$g_i(\chi_i, 0) = 0, \quad (3.42)$$

where constant  $s_i$  is unknown and found by using Newtonian's Raphson scheme such that it satisfy the condition  $f_i(\chi_i, 1) = 0$ . For  $i = 1$  the Eqs. (3.38)-(3.42) become

$$\theta_1 = f_1, \quad (3.43)$$

$$\frac{\partial \theta_1}{\partial Y} = \frac{\partial f_1}{\partial Y} = g_1, \quad (3.44)$$

$$\begin{aligned} \frac{\partial g_1}{\partial Y} = G_Z \frac{(1+\chi_1^2)^4}{2} \left[ \frac{dP_1}{d\chi_1} (Y^2 - 1) + \frac{\alpha(1+\chi_1^2)^2}{2} \left( \frac{dP_1}{d\chi_1} \right)^3 (Y^4 - \right. \\ \left. 1) + 1 \right] \frac{(f_1 - f_0)}{\Delta\chi} - Br(1 + \chi_1^2)^4 Y^2 \left( \frac{dP_1}{d\chi_1} \right)^2 \left[ 1 + \right. \\ \left. \alpha(1 + \chi_1^2)^2 Y^2 \left( \frac{dP_1}{d\chi_1} \right)^2 \right], \end{aligned} \quad (3.45)$$

$$f_1(\chi_1, 0) = s_1, \quad (3.46)$$

$$g_1(\chi_1, 0) = 0. \quad (3.47)$$

In the above equation  $f_0(-\chi_f, Y) = 0$  is an initial temperature when sheet first bite the rolls and  $s_1$  missing value, which is chosen in such a way that it satisfy the boundary condition  $f_1(\chi_1, 1) = 0$ . Now solving the Eq. (3.45) with boundary conditions Eqs. (3.46) and (3.47) we get,  $f_1$ . By continuing this technique for  $i = 2, 3, 4 \dots \dots N$ , we can find temperature at each step.

## 3.2 Results and conclusion

In this section, we explain the detail effects of Rabinowitsch fluid's non-linearity parameter on the pressure gradient, pressure, velocity profile and quantities of engineering interest such as roll separating force, power function and exiting sheet thickness and energy equation graphically. The non-linearity factor, predicts the dilatant effects for  $\alpha < 0$ , Newtonian behavior at  $\alpha = 0$  and pseudoplastic for  $\alpha > 0$ .

Fig. 3.1 and 3.2 show the dimensionless pressure gradient as a function of dimensionless axial coordinate  $\chi$  for different values of non-linear factor for lubricants,  $\alpha (= -0.5, -0.3, 0, 0.1, 0.5)$  and two fixed values of dimensionless leave off distance,  $\lambda (= 0.2923, 0.440)$ . We observe here that along the calendar gap, the pressure gradient starts from zero at  $\chi = \lambda$  then becomes negative and reaches its minimum at  $\chi = 0$ , it meets zero again at  $\chi = -\lambda$  then it becomes positive and reaches its maximum value and decreases again till  $\chi = -\chi_f$  where sheet first bites the rolls. We can see that for a given value of dimensionless leave off distance  $\lambda$ , plot of  $\alpha = 0$  is in the middle and decreasing  $\alpha$  shrinks the length of domain whereas increasing  $\alpha$  extends the length of domain. Also we observe that varying  $\alpha$  strongly effects the graph at  $\chi = 0$  because here shear rate pressure gradient has its minimum value whereas the effect is negligible near  $\chi = \lambda$  and  $\chi = -\lambda$  and we acquire flat velocity profiles here.

Fig. 3.3 and 3.4 shows the dimensionless pressure distribution which is obtained by integrating Eq. (3.22). Pressure is zero at  $\chi = \lambda$  then it increases to its maximum as  $\chi$  reaches  $-\lambda$  then pressure starts to decrease and meets zero at  $\chi = -\chi_f$  (entry point) satisfying conditions in Eqs. (3.15) and (3.16). For a given value of dimensionless leave off distance  $\lambda$  pressure has noticeable change at  $\chi = -\lambda$  as  $\alpha$  varies where change is negligible near  $\chi = \lambda$ . As pressure gradient is zero at  $\chi = -\lambda$  we can see that pressure is maximum at that point.

Fig. 3.5 and 3.6 shows the dimensionless velocity profile  $u$  as a function of transversal coordinate  $Y$  for different values of non-linear factor for lubricants  $\alpha$ . The dimensionless velocity profile is plotted for two different values of  $\chi$  in domain  $-\chi_f \leq \chi \leq -\lambda$  and  $-\lambda \leq \chi \leq \lambda$ . In the first domain decreasing the value of  $\alpha$  decreases velocity for a fixed  $\lambda$  where there is a very minor increase in velocity at locality of rolls as shown in

Fig. 3.5. In the second domain velocity increases by decreasing  $\alpha$  whereas it decreases very weakly at locality of rolls as shown in Fig. 3.6. The dimensionless velocity  $u$  for different values of  $\alpha$  (non-linear factor for lubricants) as function of dimensionless transversal coordinate  $Y$ , at  $\chi = -0.6$

In Fig. 3.7 the numerical results for dimensionless leave off distance  $\lambda$  are presented as a function of dimensionless entering sheet thickness  $H_f/H_0$ . As  $H_f/H_0$  is known in our problem so  $-\chi_f$  is calculated through relation  $\chi_f = (H_f/H_0 - 1)^{1/2}$  and we observe in Fig. 3.7 that for  $H_f/H_0 < 4.5$   $\lambda$  decreases with increase in  $\alpha$  and for  $H_f/H_0 > 4.5$ ,  $\lambda$  increases with increase in  $\alpha$ .

Quantities of engineering interest i-e the roll-separating force and power input to the fluids by the rolls are calculated and shown as a function of  $\alpha$  in Figs. 3.8 and 3.9 respectively where  $\lambda$  is varying. We can see in Fig. 3.8 that force is decreasing function of  $\alpha$  for both values of  $\lambda$ , i-e 0.2923 and 0.440. Also power in Fig. 3.9 is non-increasing function of  $\alpha$ .

Fig. 3.10-3.13 are plotted to see the effects of different parameters on the dimensionless temperature distribution at various longitudinal positions for two different values of  $\alpha$ . Figs. 3.10 and 3.11, are plotted for of  $Gz = 40$  and  $Br = 5$ . Due to the imposed boundary conditions, all the temperature profiles flatten near the center  $Y=0$  and converge to zero at the boundray  $Y=1$ . For dilatent fluids ( $\alpha < 0$ ),  $\theta(\chi, Y) < 0$  while for pseudoplastic ( $\alpha > 0$ ),  $\theta(\chi, Y) > 0$ . This clearly indicates that the temperature of the clandered sheet composed of pseudoplastic materialis higher than the temperature of the rolls. On the contrary, viscoplastic sheet made up of dilatent material has lower temperature than the temperature of the rolls. It is also observed that maximum or minimum temperature zone

appear near the vicinity of the rolls. Figs. 3.12 and 3.13 predict higher (lower) values of temperature for pseudoplastic fluid (dilatant fluids) than that observed in Figs. 3.12 and 3.13. This increase/decrease is attributed to the increase in the leave-off distance  $\lambda$ .

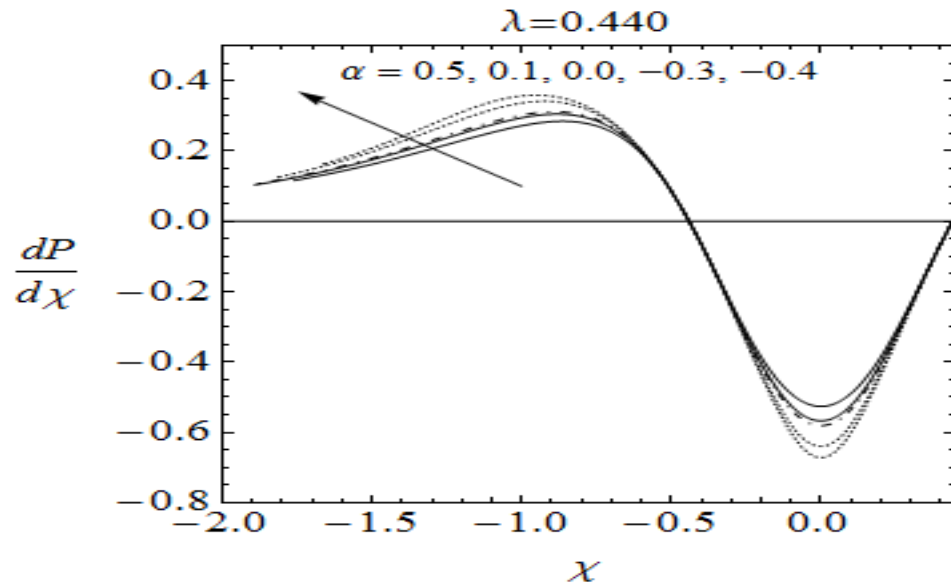


Fig. (3.1). Dimensionless pressure gradient for Rabinowitsch fluid for different values of non-linear factor for lubricants  $\alpha$  and  $\lambda = 0.440$ .

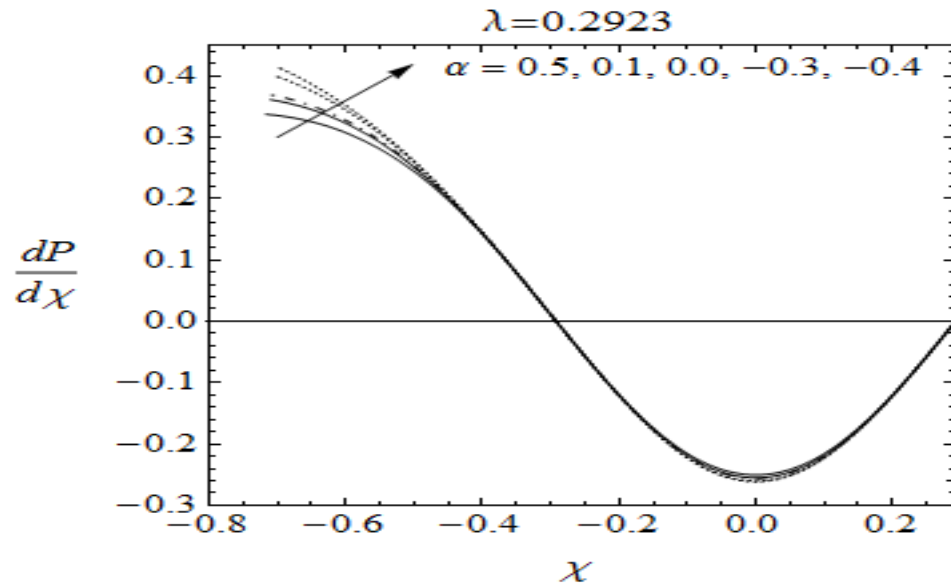


Fig. (3.2). Dimensionless pressure gradient for Rabinowitsch fluid for different values of non-linear factor for lubricants  $\alpha$  and  $\lambda = 0.2923$ .

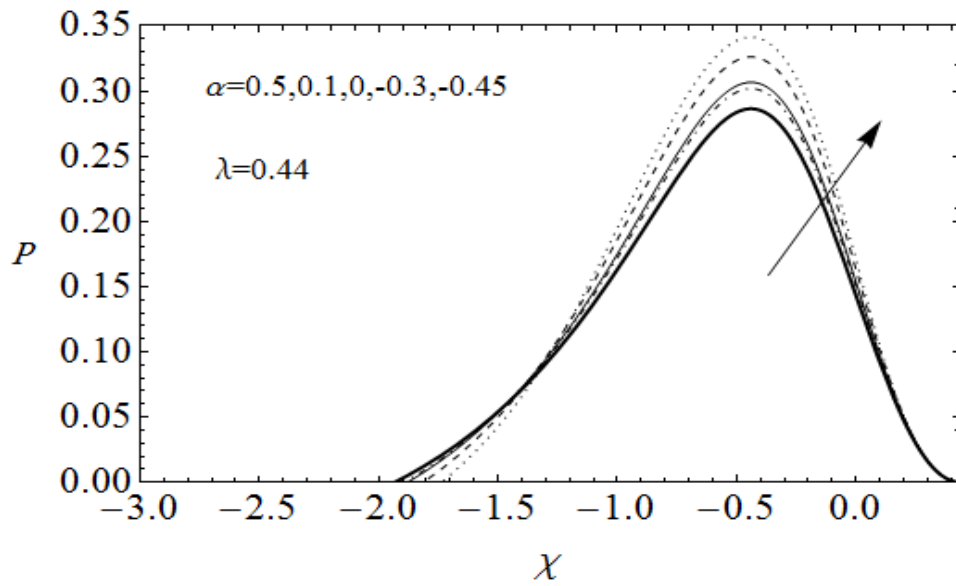


Fig. (3.3). Dimensionless pressure distribution in the gap, along the flow field for different values of  $\alpha$  and  $\lambda = 0.440$ .

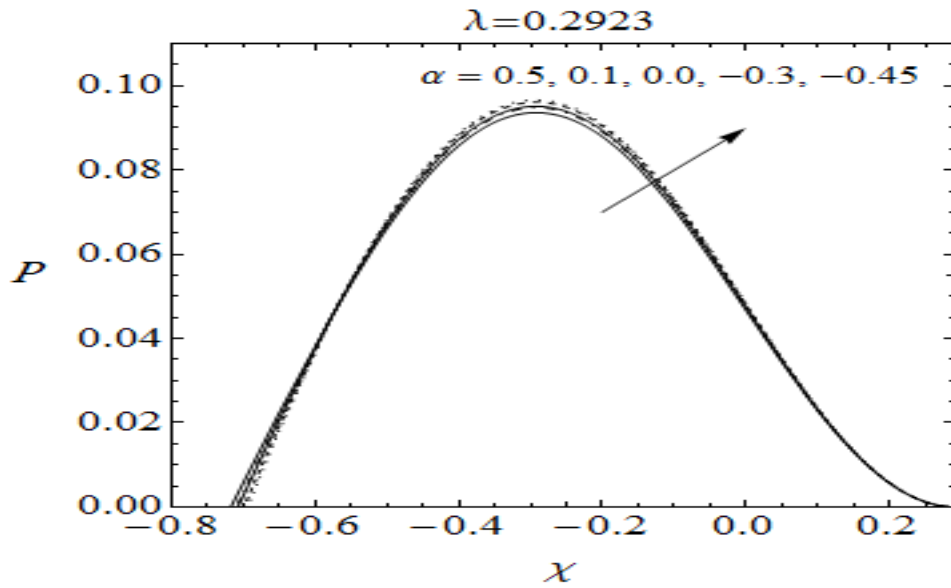


Fig. (3.4). Dimensionless pressure distribution in the gap, along the flow field for different values of  $\alpha$  and  $\lambda = 0.2923$ .



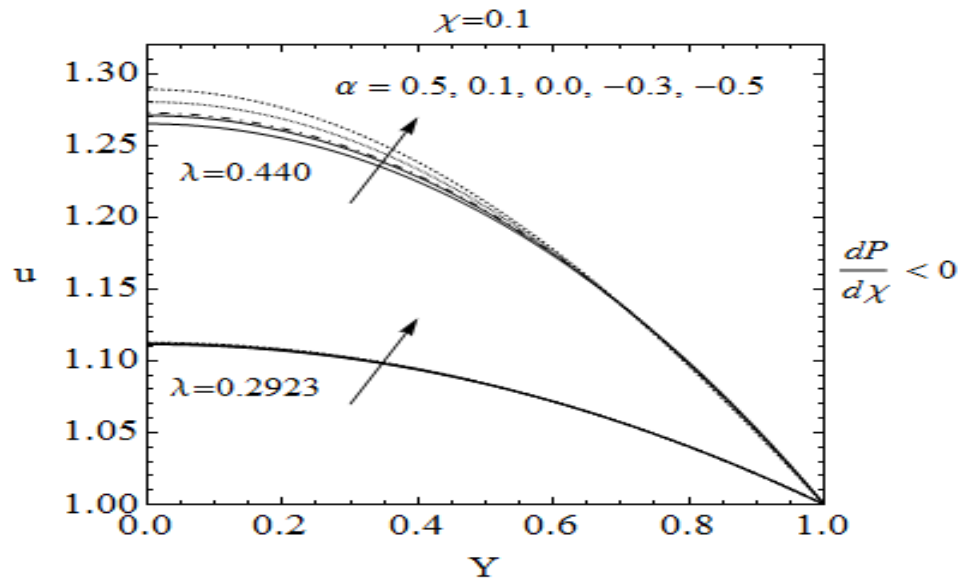


Fig.(3.5). Dimensionless Velocity  $u$  for different values of  $\alpha$  (non-linear factor for lubricants) as function of dimensionless transversal coordinate  $Y$  at  $\chi = 0.1$  and for  $\lambda = 0.440$  and  $\lambda = 0.2923$ .

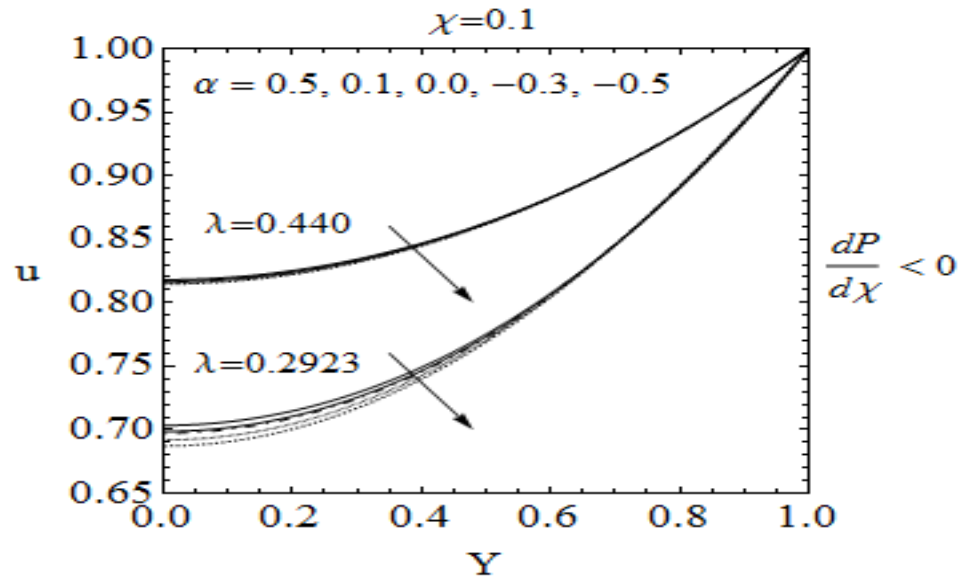


Fig. (3.6). Dimensionless Velocity  $u$  for different values of  $\alpha$  (non-linear factor for lubricants) as function of dimensionless transversal coordinate  $Y$  at  $\chi = -0.6$  and for  $\lambda = 0.440$  and  $\lambda = 0.2923$ .

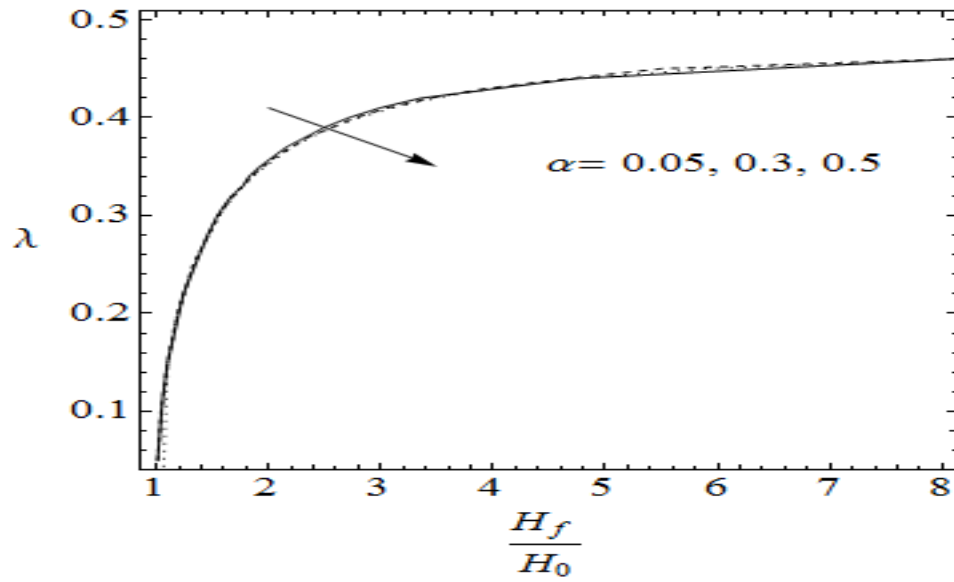


Fig. (3.7). Dimensionless leave off distance  $\lambda$  as function of entering sheet thickness  $H_f/H_0$  for different values of  $\alpha$ .

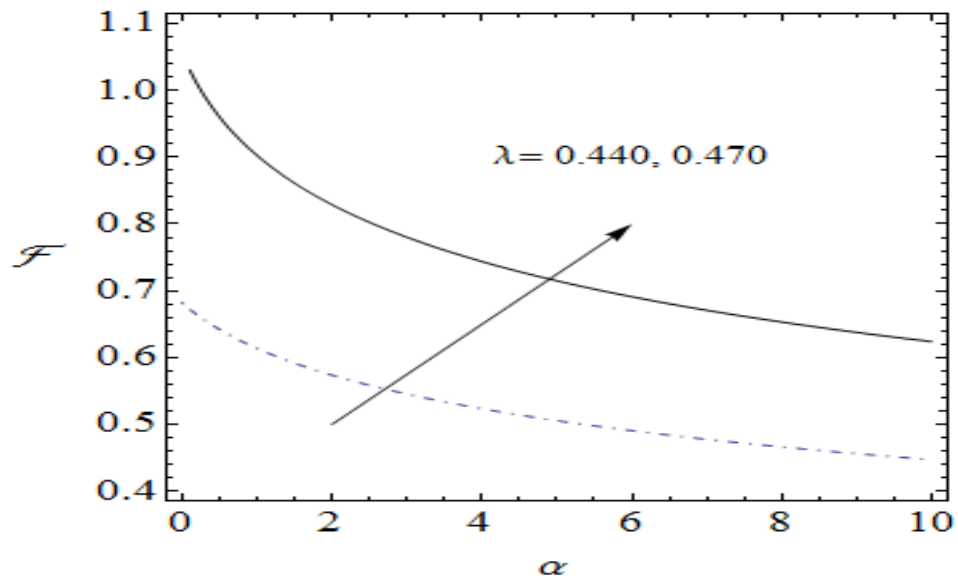


Fig. (3.8). Dimensionless force function  $F$  as function of  $\alpha$  in terms of  $\lambda$ .

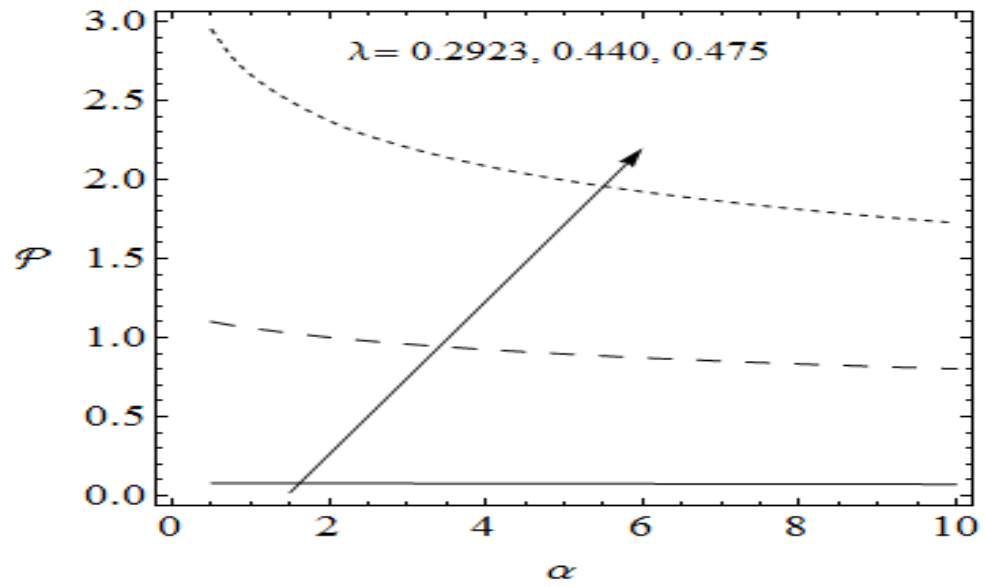


Fig. (3.9). Dimensionless power function  $P$  as function of  $\alpha$  in terms of  $\lambda$ .

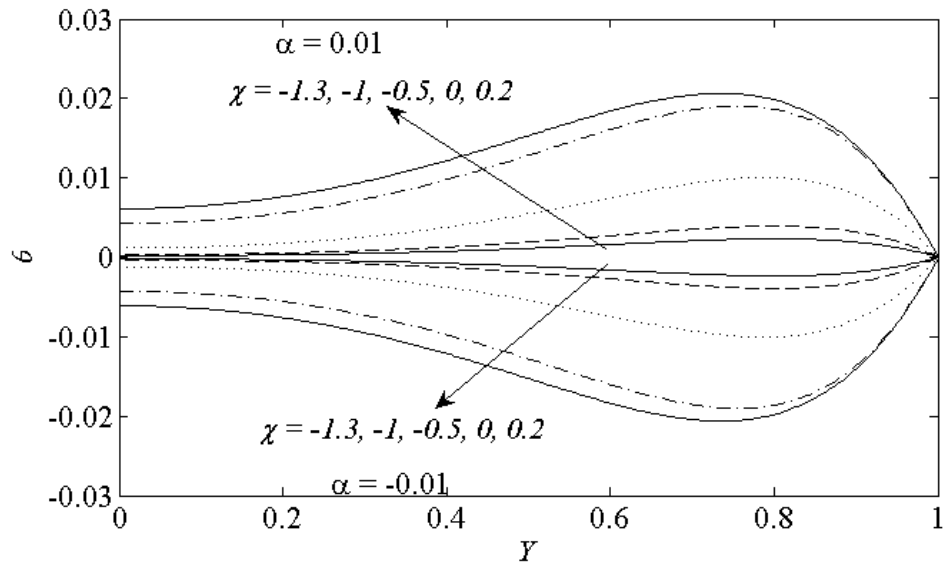


Fig. 3.10. Temperature distribution as a function of  $\chi$  and  $Y$  for five location of  $\chi$  with  $Gz = 40$ ,  $Br = 5$  and  $\lambda = 0.2923$ .

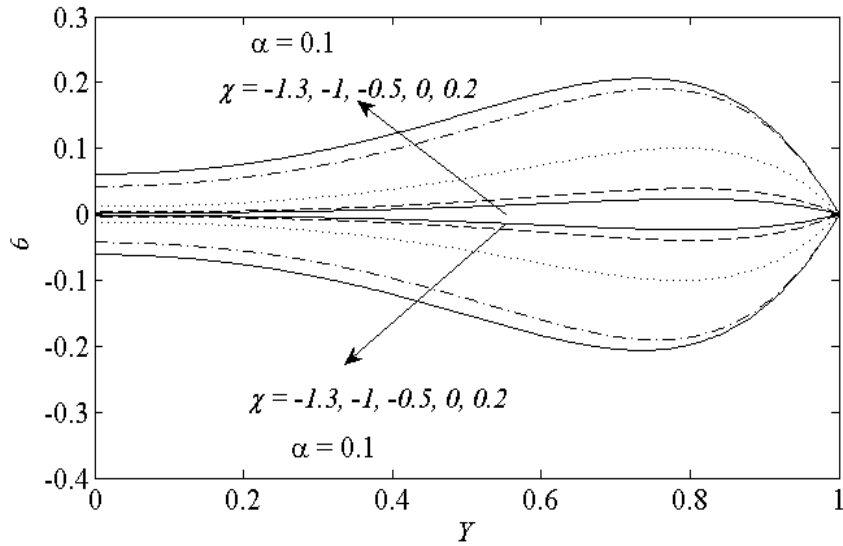


Fig. 3.11. Temperature distribution as a function of  $\chi$  and  $Y$  for five location of  $\chi$  with  $Gz = 40$ ,  $Br = 5$  and  $\lambda = 0.2923$ .

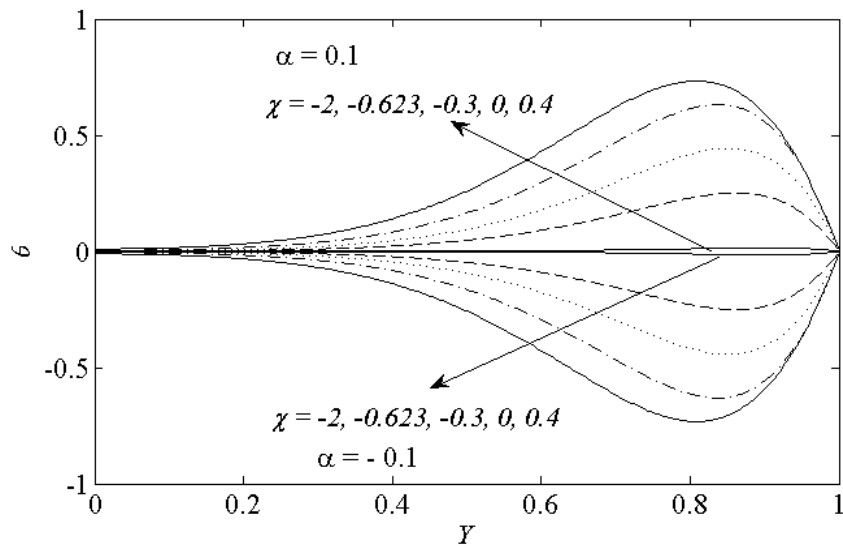


Fig. 3.12. Temperature distribution as a function of  $\chi$  and  $Y$  for five location of  $\chi$  with  $Gz = 40$ ,  $Br = 5$  and  $\lambda = 0.44$ .

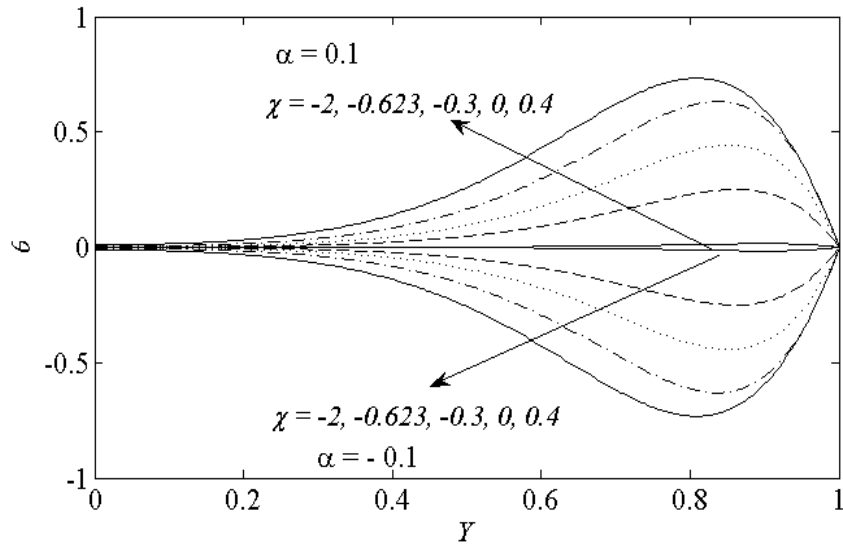


Fig. 3.13. Temperature distribution as a function of  $\chi$  and  $Y$  for five location of  $\chi$  with  $Gz = 40$ ,  $Br = 10$  and  $\lambda = 0.44$ .

## References

- [1] R.E. Gaskell, The calendering of plastic materials, *J. Appl. Mech.* 17 (1950) 334–337.
- [2] J.M. McKelvey, *Polymer Processing*, Wiley, New York, 1962.
- [3] I. Brazinsky, H.F. Cosway, C.F. Valle Jr., R Jones, R. Clark, V. Story, A theoretical study of liquid film spread heights in the calendering of Newtonian and power law fluids, *J. Appl. Polym. Sci.* 14 (1970) 2771-2784.
- [4] W. W. Alston, K. N. Astill, An Analysis for calendering of non-newtonian fluids, *J. Appl. Polym. Sci.* 17 (1973) 3157-3174.
- [5] S. Middleman, *Fundamentals of Polymer Processing*, McGraw-Hill, United States of America, 1977.
- [6] Z. Tadmor, C.G. Gogos, *Principles of Polymer Processing*, John Wiley & Sons, Haifa, Israel, 1979.
- [7] J. T. Bergen, G.W. Scott, Pressure distribution in calendering of plastic materials, *J. Appl. Mech.* 18 (1951) 101-106.
- [8] C. Kiparissides, J. Vlachopoulos, Finite element analysis of calendering, *Polym. Eng. Sci.* 16 (1976) 712-719.
- [9] C. Kiparissides, J. Vlachopoulos, A study of viscous dissipation in the calendering of power-law fluids, *Polym. Eng. Sci.* 18 (1978) 210–214.
- [10] M. Finston, Thermal effects in calendering of plastic materials, *J. Appl. Mech.* 18 (1951) 12-20.
- [11] P. R. Pasley, Calendering of viscoelastic materials, *J. Appl. Mech.* 24 (1957) 602-608.

- [12] N. Tokita, J. L. White, Milling behavior of gum elastomers: Experiment and theory, *J. Appl. Polym. Sci.* 10 (1966) 1011-1026.
- [13] J. S. Chong, Calendering thermoplastic materials, *J. Appl. Polym. Sci.* 12 (1968) 191-212.
- [14] S. Sofou, E. Mitsoulis, Calendering of pseudoplastic and viscoplastic sheets of finite thickness, *J. Plastic Film Sheet.* 20 (2004) 185–222.
- [15] E. Mitsoulis, J. Vlachopoulos, F. A. Mirza, Calendering analysis without the lubrication approximation, *Polym. Eng. Sci.* 25 (1985) 6-18.
- [16] J. P. Agassant, M. Espy, Theoretical and experimental study of the molten polymer flow in the calender bank, *Polym. Eng. Sci.* 25 (1985) 113-121.
- [17] E. Mitsoulis, Numerical simulation of calendering viscoplastic fluids, *J. Non-Newton. Fluid Mech.* 154 (2008) 77-88.
- [18] R. Zheng, R. I. Tanner, A Numerical analysis of calendering, *J. Non-Newton. Fluid Mech.* 28 (1988) 149-170.
- [19] J.C. Arcos, F. Méndez, O. Bautista, Effect of temperature-dependent consistency index on the exiting sheet thickness in the calendering of power-law fluids, *Int. J. Heat Mass Transfer*, 54 (2011) 3979–3986.
- [20] J.C. Arcos, O. Bautista, F. Mendez, Theoretical analysis of the calendered exiting thickness of viscoelastic sheets, *J. Non-Newton. Fluid Mech.* (2012) 29-36.
- [21] J.C. Arcos, J. E. Munoz, O. Bautista, F. Mendez, Corrigendum to “Theoretical analysis of the calendered exiting thickness of viscoelastic sheets”, *J. Non-Newton. Fluid. Mech.* (2016) 1-4.

- [22] A. M. Siddiqui, M. Zahid, M. A. Rana, T. Haroon, Calendaring analysis of third order fluid, *J. Plastic Film Sheet.* 30 (2014) 345-368.
- [23] M. Zahid, M. A. Rana, A. M. Siddiqui, T. Haroon, Modeling of non-isothermal flow of a magnetohydrodynamic, viscoplastic fluid during calendaring, *J. Plastic Film Sheet*, (2015) 1-24.
- [24] N. Ali, M. A. Javed, M. Sajid, Theoretical analysis of exiting sheet thickness of sheets in the calendaring of Fene-P fluid, *J. Non-Newton. Fluid. Mech.* 225 (2015) 28-36.
- [25] M.Sajid, N. Ali, M.A. Javed, An exact solution for calendaring analysis of third order fluid, *J. Plastic Film Sheeting*, 0(0) 2016 1-18.
- [26] J.F. Wendt, *Computational Fluid Dynamics*, Springer, 2009.
- [27] J. D. Hoffman, *Numerical methods for engineers and scientists*, CRC press, New York 2001.